The Plant Cell, Vol. 31: 1257–1275, June 2019, www.plantcell.org © 2019 ASPB.

OsSPL3, an SBP-Domain Protein, Regulates Crown Root Development in Rice[OPEN]

Yanlin Shao,[a] Hong-Zhu Zhou,[a] Yunrong Wu,[a] Hui Zhang,[b] Jian Lin,[a] Xiaoyan Jiang,[a] Qiuju He,[a] Jianshu Zhu,[a] Yong Li,[a] Hao Yu,[c] and Chuanzao Mao[a,1]

[a] State Key Laboratory of Plant Physiology and Biochemistry, College of Life Sciences, Zhejiang University, Hangzhou 310058, China
[b] College of Bioscience and Biotechnology, Yangzhou University, Yangzhou 225009, China
[c] Department of Biological Sciences and Temasek Life Sciences Laboratory, National University of Singapore, 117543, Singapore

ORCID IDs: 0000-0002-7211-6569 (Y.S.); 0000-0001-9318-335X (H.-Z.Z.); 0000-0002-4579-0021 (Y.W.); 0000-0001-8904-0233 (H.Z.); 0000-0001-7394-0528 (J.L.); 0000-0002-4323-9279 (X.J.); 0000-0001-5589-3684 (Q.H.); 0000-0002-4877-8773 (J.Z.); 0000-0003-0811-462X (Y.L.); 0000-0002-9778-8855 (H.Y.); 0000-0001-5126-2180 (C.M.)

The major root system of cereals consists of crown roots (or adventitious roots), which are important for anchoring plants in the soil and for water and nutrient uptake. However, the molecular basis of crown root formation is largely unknown. Here, we isolated a rice (*Oryza sativa*) mutant with fewer crown roots, named *lower crown root number1* (*lcrn1*). Map-based cloning revealed that *lcrn1* is caused by a mutation of a putative transcription factor–coding gene, *O. sativa SQUAMOSA PROMOTER BINDING PROTEIN-LIKE3* (*OsSPL3*). We demonstrate that the point mutation in *lcrn1* perturbs the*O. sativa* microRNA156 (OsmiR156)-directed cleavage of *OsSPL3* transcripts, resulting in the mutant phenotype. Chromatin immunoprecipitation sequencing assays of OsSPL3 binding sites and RNA sequencing of differentially expressed transcripts in *lcrn1* further identified potential direct targets of OsSPL3 in basal nodes, including a MADS-box transcription factor, OsMADS50. *OsMADS50*-overexpressing plants produced fewer crown roots, phenocopying *lcrn1*, while knocking out *OsMADS50* in the *lcrn1* background reversed this phenotype. We also show that *OsSPL12*, another OsmiR156 target gene, regulates *OsMADS50* and crown root development. Taken together, our findings suggest a novel regulatory pathway in which the OsmiR156-*OsSPL3*/*OsSPL12* module directly activates *OsMADS50* in the node to regulate crown root development in rice.

INTRODUCTION

Roots anchor plants in the soil and mediate water and nutrient uptake. Root system architecture describes the shape and spatial arrangement of a root system within the soil (Rogers and Benfey, 2015). The root system is shaped by the interactions between genetic and environmental components that form a framework for the plant to explore the soil and respond to external cues. For example, the model dicot Arabidopsis (*Arabidopsis thaliana*) rarely generates adventitious roots (Smith and De Smet, 2012; Xu et al., 2016), whereas monocots produce numerous adventitious roots that emerge from the stem nodes of cereals and are referred to as crown roots (Marcon et al., 2013). How crown roots form is poorly understood. Identifying the molecular determinants that regulate crown root development is an important step toward improving root system architecture to enhance yields and nutrient uptake efficiency (White et al., 2013).

Genetic studies first suggested that genes involved in auxin signaling play important roles in crown root development in rice (*Oryza sativa*). The first identified gene was *ADVENTITIOUS ROOTLESS1*/*CROWN ROOTLESS1* (*ARL1*/*CRL1*), which encodes a LATERAL ORGAN BOUNDARIES domain transcription factor (Inukai et al., 2005; Liu et al., 2005). The *arl1* mutant produces no adventitious roots and adventitious root primordia throughout its life cycle, although its aboveground organs are normal (Liu et al., 2005). Further study indicated that *ARL1*/*CRL1* is a direct target of AUXIN RESPONSE FACTOR1 (OsARF1), which can be induced by exogenous auxin treatment (Inukai et al., 2005; Liu et al., 2005). *CRL4*/*OsGNOM1*, encoding a guanine nucleotide exchange factor of the ADP-ribosylation factor family, affects crown root formation by regulating polar auxin transport (Kitomi et al., 2008; Liu et al., 2009), while RNA interference of *PIN-FORMED1* (*OsPIN1*), an auxin efflux transporter, inhibits adventitious root development (Xu et al., 2005). AUXIN/INDOLE-3-ACETIC ACID (IAA) proteins function as ARF inhibitors, preventing auxin signaling. The gain-of-function mutant *osiaa23*, which accumulates the auxin response protein OsIAA23, shows defects in the initiation of crown and lateral roots (Jun et al., 2011). Furthermore, *CULLIN-ASSOCIATED AND NEDDYLATION-DISSOCIATED1* (*OsCAND1*), a gene involved in the auxin signaling pathway that regulates the G2/M cell cycle transition, is required for crown root emergence in rice (Wang et al., 2011b). Thus, genes involved in auxin signaling play important roles in crown root development.

Cytokinins (CKs), a class of hormones that act antagonistically to auxin, are also essential for crown root development in rice. The *WUSCHEL-RELATED HOMEOBOX* (*WOX*) gene, *OsWOX11*, is an important player in CK-regulated crown root development in rice (Zhao et al., 2009, 2015, 2017); the loss of *OsWOX11* function results in a significant reduction in the number of crown roots, whereas the overexpression of this gene substantially promotes

[1] Address correspondence to mcz@zju.edu.cn.
The author(s) responsible for distribution of materials integral to the findings presented in this article in accordance with the policy described in the Instructions for Authors (www.plantcell.org) is: Chuanzao Mao (mcz@zju.edu.cn).
[OPEN]Articles can be viewed without a subscription.
www.plantcell.org/cgi/doi/10.1105/tpc.19.00038

crown root growth. OsWOX11 directly represses *O. sativa RESPONSE REGULATOR2* (*OsRR2*), a type-A CK-responsive gene expressed in the crown root primordia, by binding to its promoter (Zhao et al., 2009). *O. sativa* ETHYLENE-RESPONSIVE FACTOR3 (OsERF3) also regulates the expression of *OsRR2* during crown root initiation and likely interacts with OsWOX11 to repress *OsRR2* expression during crown root elongation (Zhao et al., 2015). The expression of *CRL5*, which encodes an APETELA2/ERF transcription factor, can be induced by exogenous auxin. The *crl5* mutant produces fewer crown roots because the initiation of its crown root primordia is impaired. CRL5 upregulates the expression of the type-A CK response regulator *OsRR1*, which represses CK signaling to regulate crown root initiation in rice (Kitomi et al., 2011). These data indicate that crown root development is coordinately regulated by auxin and CK signaling. Although many genes involved in rice crown root development have been identified, our knowledge of this process is still fragmented.

SQUAMOSA PROMOTER BINDING PROTEIN-LIKEs (SPLs) are plant-specific transcription factors (Klein et al., 1996). There are 19 *SPL* genes in rice; they are classified into six subgroups (Xie et al., 2006). To date, five genes (*OsSPL6*, *OsSPL8*, *OsSPL13*, *OsSPL14*, and *OsSPL16*) of the 19 *SPL* genes in rice have been identified that play roles in plant architecture; inflorescence architecture; panicle apical abortion; and grain size, shape, and quality (Lee et al., 2007; Jiao et al., 2010; Miura et al., 2010; Wang et al., 2012, 2018b; Si et al., 2016). However, the biological functions of other *SPL* genes in rice are largely unknown.

In this study, we isolated the *lower crown root number1* (*lcrn1*) mutant and cloned and identified *LCRN1*, which encodes OsSPL3. A point mutation in *OsSPL3* perturbed the *O. sativa* microRNA156 (OsmiR156)–directed cleavage of the *OsSPL3* transcripts in *lcrn1*, resulting in a decrease in the number of crown roots. By combining chromatin immunoprecipitation sequencing (ChIP-seq) and RNA-seq approaches, we further demonstrate that *OsMADS50*, is the direct target of OsSPL3. *OsMADS50*-overexpressing lines produced fewer crown roots, similar to *lcrn1*, while knocking out *OsMADS50* function in *lcrn1* rescued its crown root phenotype, suggesting that *OsMADS50* is a direct target of OsSPL3. Our results support a model in which the OsmiR156-*OsSPL3/OsSPL12* module directly activates *OsMADS50* in the node to regulate crown root development in rice.

RESULTS

The *lcrn1* Mutant Produces Fewer Crown Roots

In a screen of adventitious root–related mutants, one mutant with reduced crown roots was isolated from an ethyl methanesulfonate (EMS)–mutated mutant library. The mutant was named *lcrn1*^{Kas}, for *lcrn1* in the Kasalath (Kas) background, according to its phenotype. Five-day-old *lcrn1*^{Kas} did not have any crown roots, while the wild-type Kas plants had formed two to four crown roots by the same developmental stage (Supplemental Figure 1A). *lcrn1*^{Kas} did produce crown roots at later stages; however, this mutant had fewer crown roots than the wild type at all developmental stages; 5-week-old *lcrn1*^{Kas} had ~43% of the number of crown roots produced by the wild type (21.5 versus 50.2; Supplemental Figure 1B).

We examined the root gravitropic response in *lcrn1*^{Kas} by measuring the curvature of root growth after rotating the seedling 90°. The root tip angle of *lcrn1*^{Kas} (average 50.2 ± 6.6°) was significantly smaller than that of the wild type (average 63.4 ± 6.2°; Supplemental Figures 1C and 1D), suggesting that the root gravitropic response was impaired in *lcrn1*^{Kas}. When treated with IAA or naphthalene acetic acid (NAA), the crown root number of the wild type increased in a dose-dependent manner up to 10^{-7} M IAA or 10^{-9} M NAA and then was inhibited at higher concentrations. The stimulatory effect of exogenous auxin was not observed in *lcrn1*^{Kas} at the same auxin concentration; however, the crown roots were observable in *lcrn1*^{Kas} treated with 10^{-5} M IAA or 10^{-7} M NAA and even more crown roots were observed in plants treated with 10^{-5} M NAA (Supplemental Table). This observation suggests that *lcrn1*^{Kas} is less sensitive to auxin treatment compared with the wild type.

To shorten the mutant growth period, we crossed the mutant with a short growth period variety, Hei Jing 2 ([HJ2], cv *japonica*), and backcrossed it eight times with HJ2 to generate the BC_8F_3 mutant allele in the HJ2 genetic background (hereafter named *lcrn1*). Five-day-old *lcrn1* mutant seedlings had normal primary root development, but did not form any visible crown roots, whereas the wild-type (HJ2) plants had formed three to five crown roots by the same stage (Figures 1A and 1B). The *lcrn1* seedlings began to generate visible crown roots 8 d after germination (DAG). Further investigation of crown root numbers of the wild type and *lcrn1* at different developmental stages revealed that *lcrn1* had significantly fewer crown roots than the wild type at each growth stage (Figure 1B). After 47 d, the number of crown roots produced by *lcrn1* was ~46% of that of the wild type (60.6 versus 131.2; Figure 1B). Cross sections of the stem bases showed that the normal crown root primordia had initiated in the coleoptilar node in the 36-h-old mutant and the wild type seedlings. The size of crown root primordia of the mutant was smaller than that of the wild type in 48- and 72-h-old seedlings; furthermore, fewer crown root primordia were produced by the mutant (2.3 on average) compared with the wild type (3.5 on average) in 72-h-old seedlings (Figures 1C and 1D). These results suggested that the crown root primordia initiation and development were slower in the *lcrn1* mutant than in the wild type.

The *lcrn1* mutant also had a slightly reduced plant height compared with the wild type (Supplemental Figure 2A) and produced fewer tillers (Supplemental Figure 2B) and fewer lateral roots (Supplemental Figure 2C), but did not alter the length of the lateral root (Supplemental Figure 2D).

LCRN1 Encodes OsSPL3, a Predicted Transcription Factor

LCRN1 was mapped onto chromosome 2 of the rice genome, between simple sequence repeat markers RM5764 and RM279, using an F_2 population derived from a cross between *lcrn1*^{Kas} and HJ2. *LCRN1* was further fine-mapped into a 625-kb region between markers RM5764 and S02-2200k (Figure 2A). A subsequent resequencing of the mutant and wild-type genomes revealed a single nucleotide substitution (C to T; 1157 bp from the start codon of the coding sequence [CDS]) in the fourth exon of *OsSPL3* (LOC_Os02g04680.1) in *lcrn1*^{Kas}. This mutation caused an amino acid change from Ser to Phe in the *lcrn1*^{Kas} mutant (Figure 2A).

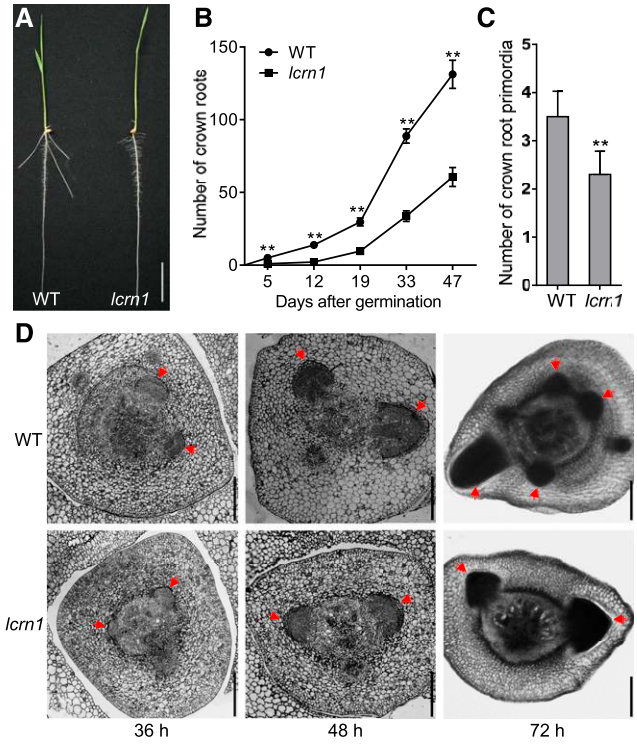

Figure 1. Phenotype of *lcrn1*.

(A) Wild-type (HJ2) and *lcrn1* seedlings at 5 d. Bar = 3 cm. WT, wild type.
(B) Number of crown roots produced by the wild-type and *lcrn1* plants throughout development. Data are shown as means ± SD (n = 20 independent plants). **Significant difference between the wild type and *lcrn1* ($P < 0.01$; Student's t test). WT, wild type.
(C) Number of crown root primordia in the coleoptilar node of 72-h wild-type and *lcrn1* seedlings. Data are shown as means + SD (n = 10 independent plants). **Significant difference between wild type and *lcrn1* ($P < 0.01$; Student's t test). WT, wild type.
(D) Cross sections of the coleoptilar node of the wild-type and *lcrn1* seedlings at 36, 48, or 72 h after germination. Red arrows indicate crown root primordia. Bars = 200 μm. WT, wild type.

OsSPL3 contains four exons and three introns, with a CDS of 1410 bp (Figure 2A) and is predicted to encode a SQUAMOSA PROMOTER BINDING PROTEIN (SBP)-domain transcription factor of 469 amino acids.

Interestingly, sequence alignment revealed that the coding region of *OsSPL3* contains an OsmiR156-complementary sequence and that the *lcrn1* mutation was located within the OsmiR156-target site (Supplemental Figure 3). miRNAs generally direct the cleavage of complementary mRNAs in plants. To investigate whether the nucleotide substitution (C to T) in *OsSPL3* in the *lcrn1* mutant affects the abundance of *OsSPL3* transcripts, we performed quantitative real-time PCR analysis and found that *OsSPL3* transcript levels were much higher (~20-fold greater) in the basal node of 3-d-old *lcrn1* seedlings than in the wild type (Figure 2B). Further analyses of *OsSPL3* expression revealed its higher expression in *lcrn1* plants than in the wild type in all tissues examined at the rice heading stage (Figure 2C).

To determine whether the mutation in *OsSPL3* underlies the *lcrn1* mutant phenotype, we cloned a 7.0-kb HJ2 genomic DNA fragment containing the 3.2-kb promoter sequence upstream of *OsSPL3*, the *OsSPL3* gene sequence, and the 0.5-kb sequence downstream of the *OsSPL3* stop codon and mutated the *OsSPL3* gene sequence by replacing the nucleotide C to T at 1157 bp along the CDS. The mutated *OsSPL3* was named *OsmSPL3* and transformed into HJ2. The resultant transgenic lines were named *OsmSPL3*^{HJ2}. Like the *lcrn1* mutant, the *OsmSPL3*^{HJ2} plants produced fewer crown roots than the wild type (Figure 2D). Consistently, the expression of *OsSPL3* was strongly elevated in *OsmSPL3*^{HJ2} plants (Figure 2E).

Sequencing analysis revealed the presence of nine single-nucleotide polymorphisms (SNPs) and one indel between HJ2 and Kas in the *OsSPL3* genomic region. To confirm the function of the *OsmSPL3* allele in the Kas background, we amplified the 7.0-kb *OsSPL3* region from *lcrn1*^{Kas} and transformed it into HJ2, generating transgenic lines named *OsmSPL3*^{Kas}. Like the *lcrn1* mutant and the *OsmSPL3*^{HJ2} transgenic lines, the *OsmSPL3*^{Kas} transgenic lines also formed fewer crown roots than the wild type and had elevated *OsSPL3* transcript levels (Supplemental Figure 4).

Taken together, we concluded that the single nucleotide substitution of *OsSPL3* in the *lcrn1* mutant resulted in elevated expression of *OsSPL3* and caused the *lcrn1* phenotype.

The Point Mutation in *OsSPL3* Perturbs Its OsmiR156-Mediated Cleavage in *lcrn1*

To determine whether *OsSPL3* could be regulated by OsmiR156 in vivo, we mapped the OsmiR156-directed cleavage sites of *OsSPL3* using RNA ligase–mediated rapid amplification of cDNA ends (RLM-RACE). Sequencing 33 randomly selected clones revealed that their 5′ ends were the cleaved fragment ends from the middle of the OsmiR156-target site, where the single nucleotide substitution was located in *lcrn1* (Figure 3A).

An analysis of the expression patterns of *OsSPL3* and OsmiR156 in various rice organs and different developmental stages showed that *OsSPL3* expression was low in the basal nodes at the early seedling stage but high in the basal nodes and elongated nodes at the heading stage, which contrasted with the expression pattern of OsmiR156 (Supplemental Figure 5A). Consistent with this antagonistic pattern, the interruption of OsmiR156 function by the overexpression of the OsmiR156-target mimic *ProUBI:MIM156* resulted in increased levels of *OsSPL3* transcripts and transcripts encoding other SPLs (Supplemental Figure 5B). These results indicated that *OsSPL3* was posttranscriptionally downregulated by OsmiR156-directed cleavage in vivo. Sequencing the reverse transcription PCR (RT-PCR) products encompassing the cleavage site in the heterozygous plants indicated that the *OsSPL3* mRNAs were mainly present in the mutated form (21 of 23 sequenced clones; Supplemental Figure 6). These results suggest that the single nucleotide substitution in *OsSPL3* in the *lcrn1* mutant perturbed the OsmiR156-mediated cleavage of the *OsSPL3* transcripts.

To confirm that the *lcrn1* mutant phenotype was caused by the perturbed OsmiR156-mediated cleavage of the *OsSPL3*

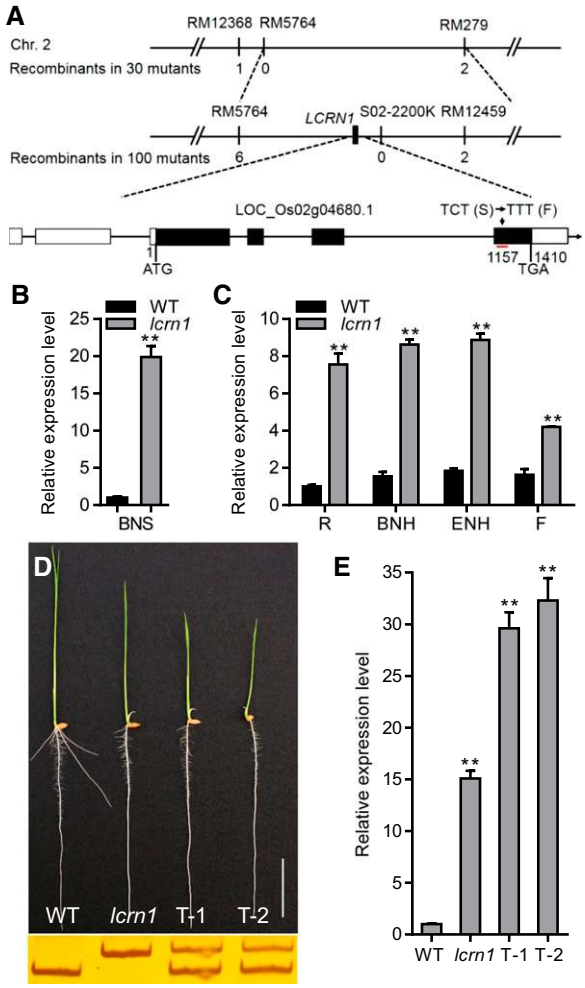

Figure 2. Map-Based Cloning of *LCRN1*.

(A) Map-based cloning of *LCRN1*. Numbers below the molecular markers indicate the number of recombinant(s) in the *lcrn1*^{Kas}/HJ2 F_2 population. The gene structure of *LCRN1* and the *lcrn1* point mutation are presented at the bottom. In the gene schematic, the black boxes represent exons and the lines between them represent introns, while the white boxes indicate untranslated regions. The red line indicates the target site of OsmiR156. Chr., chromosome; RM., simple sequence repeat marker; CTC (S)., nucleotide CTC in the CDS (Ser); TTT (F)., nucleotide TTT in the CDS (phenylalanine).

(B) and **(C)** Quantitative real-time PCR analysis of the relative expression of *OsSPL3* in the basal nodes of 3-d-old wild-type (WT) and *lcrn1* plants **(B)** and in different organs of WT and *lcrn1* plants at the heading stage **(C)**. Data were normalized to that of the WT (which was set to 1) in **(B)** and to that of the WT root (which was set to 1) in **(C)**. Values are shown as means + SD ($n = 3$ independent pools of tissue, five plants per pool). **Significant difference between WT and *lcrn1* ($P < 0.01$; Student's *t* test). BNS, basal nodes of 3-d-old seedlings; BNH, basal nodes at heading stage; ENH, elongated nodes at heading stage; F, flower; R, root at heading stage.

(D) Phenotype of 5-d-old *OsmSPL3*^{HJ2} transgenic plants (top) and the results of the derived cleaved amplified polymorphic sequence marker for the WT, *lcrn1*, and two *OsmSPL3*^{HJ2} transgenic plants (T-1 and T-2; bottom). Bar = 3 cm.

(E) Quantitative real-time PCR analysis of the relative expression of *OsSPL3* in the 5-d-old wild-type (WT), *lcrn1*, and two *OsmSPL3*^{HJ2} transgenic plants (T-1 and T-2). Data were normalized to those of the WT (the level of WT was set to 1). Values are shown as means + SD (n = 3 independent pools of seedlings, three plants per pool). **Significant difference compared with WT ($P < 0.01$; Student's *t* test).

transcripts rather than by the function of an aberrant OsSPL3 protein, we generated *ProSPL3*:*smSPL3* and *ProSPL3*:*SPL3* constructs, with and without synonymous mutations in the OsmiR156-target site, respectively, and transformed these constructs into HJ2 (Figure 3B). Crown root initiation was inhibited in the *ProSPL3*:*smSPL3* transgenic plants possessing the synonymous mutation in the OsmiR156-target site; by contrast, the *ProSPL3*:*SPL3* transgenic plants lacking any mutation in the OsmiR156-target site showed no observable phenotypic difference from that of the wild type (Figure 3C). A quantitative real-time PCR analysis showed that the transcript levels of *OsSPL3* were significantly elevated in the *ProSPL3*:*smSPL3* transgenic plants but were much lower in the *ProSPL3*:*SPL3* transgenic plants than in *lcrn1* (Figure 3D).

Thus, we concluded that the single nucleotide substitution in *OsSPL3* perturbed the OsmiR156-mediated cleavage of the *OsSPL3* transcripts, resulting in the accumulation of *OsSPL3* transcripts in the *lcrn1* mutant.

Expression Pattern of *OsSPL3*

To further investigate the expression pattern of *OsSPL3*, transgenic plants harboring a β-glucuronidase (*GUS*) reporter gene driven by the *OsSPL3* promoter (the 3.2-kb sequence upstream of the start codon) were produced. Histochemical staining for GUS activity in the T2 seedlings revealed that *OsSPL3* was mainly expressed in the stem base, primary root, crown roots, and lateral roots, with the highest level of expression in the root tips (Figures 4A to 4F), consistent with the results of the quantitative real-time PCR analysis (Figures 2B and 2C). *OsSPL3* was expressed in the epidermis, exodermis, sclerenchyma, endodermis, and stele of the primary root maturation zone (Figure 4C). *OsSPL3* was highly expressed in the root cap and the meristematic zone of the root tip (Figure 4F).

To visualize *OsSPL3* expression in the crown root primordia, transgenic plants containing an *OsSPL3* promoter–driven green fluorescent protein (GFP) reporter gene were generated. GFP fluorescence was detected in the crown root primordia, the peripheral cylinder of the vascular bundles, and the leaf sheath cells (Figure 4G).

To test the effect of the point mutation on OsSPL3 protein level, we produced transgenic plants expressing an *SPL3-GFP* fusion with (*ProSPL3*:*smSPL3-GFP*) or without (*ProSPL3*:*SPL3-GFP*) a synonymous mutation in the OsmiR156-target sequence, driven by the *OsSPL3* promoter. The *ProSPL3*:*smSPL3-GFP* transgenic plants had a similar root phenotype as the *lcrn1* mutant, indicating that the fusion protein was functionally identical to OsSPL3 (Supplemental Figure 7A). Transgenic plants lacking the mutation in the OsmiR156-target site had no observable GFP fluorescence in the crown root primordia or the peripheral cylinder (Figure 4H); by contrast, the transgenic plants containing the mutated OsmiR156-target site showed strong GFP fluorescence in the crown root primordia (Figures 4I and 4J). Furthermore, substantially increased

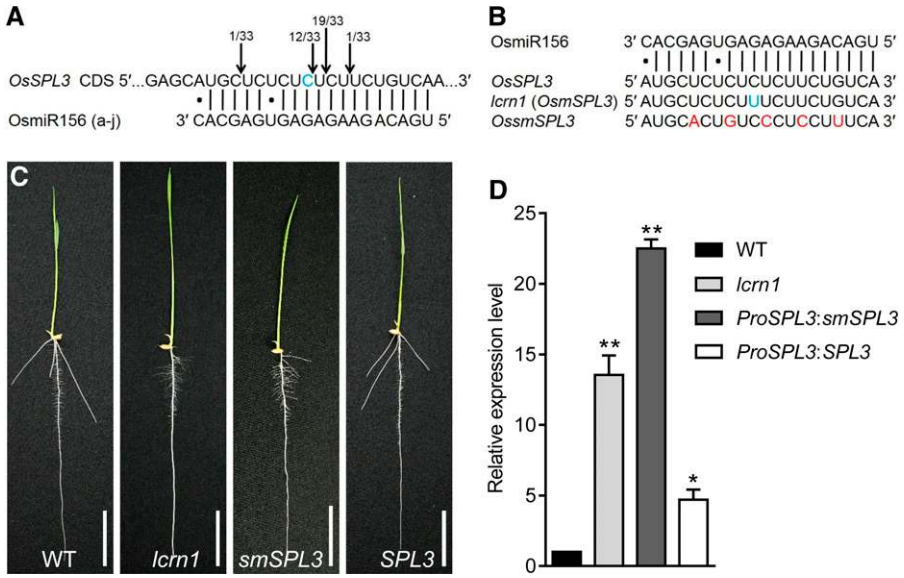

Figure 3. Confirmation of the OsmiR156-Mediated Posttranscriptional Regulation of *OsSPL3*.

(A) OsmiR156 cleavage sites in *OsSPL3* mRNA, determined using an RLM-RACE. The vertical lines represent the nucleotides that base pair with OsmiR156 and the dots show mismatched nucleotides. The positions corresponding to the 5′ ends of the cleaved *OsSPL3* mRNAs determined using 5′ RACE, and the number of 5′ RACE clones corresponding to each site are indicated. The blue nucleotide indicates the mutation site in the *lcrn1* mRNA.

(B) Synonymous mutations in the OsmiR156-target site of *OssmSPL3*. The blue nucleotide indicates the mutation site in the *lcrn1* mRNA. The red letters indicate mutated nucleotides introduced into the OsmiR156-target site in the *ProSPL3*:*smSPL3* (*smSPL3*) transgene, which altered the mRNA sequence without changing the amino acid residues it encodes.

(C) Phenotypes of the wild-type, *lcrn1*, *ProSPL3*:*smSPL3* (*smSPL3*), and *ProSPL3*:*SPL3* (*SPL3*) transgenic plants. Bar = 3 cm. WT, wild type.

(D) Quantitative real-time PCR analysis of the transcript levels of *OsSPL3* in the 5-d-old wild-type (WT), *lcrn1*, *ProSPL3*:*smSPL3*, and *ProSPL3*:*SPL3* transgenic plants. Data were normalized to that of the WT (the level of WT was set to 1). Values are means + SD ($n = 3$ independent pools of seedlings, three plants per pool). Significant difference compared with WT (*$P < 0.05$; **$P < 0.01$; Student's *t* test).

levels of OsSPL3 protein were detected in the *ProSPL3*:*smSPL3-GFP* transgenic plants, but not in the *ProSPL3*:*SPL3-GFP* transgenic plants (Supplemental Figure 7C). These results suggest that *OsSPL3* is expressed in the crown root primordia and that the mutation in the OsmiR156-target site leads to the accumulation of OsSPL3 in these cells.

OsSPL3 Is a Functional Transcription Factor

In the basal node and root tip of *ProSPL3*:*smSPL3-GFP* transgenic plants, the GFP signal was detected mainly in the nuclei (Figures 4J and 5A), which is consistent with its predicted role as a transcription factor. To determine whether OsSPL3 has transcription-activating activity, fragments of OsSPL3 with or without the SBP domain, N-terminal region, or C-terminal region were assayed in yeast (*Saccharomyces cerevisiae*) cells. Yeast cells transformed with the N-terminal 70 amino acids or N-terminal 181 amino acids can grow on selective media. The results indicated that OsSPL3 had transcription-activating activity, with the activation domain located in the first 70 amino acids of the N terminus (Figure 5B). Yeast cells transformed with the full-length CDS did not grow (Figure 5B) and showed no detectable fusion protein (Supplemental Figure 8), suggesting that full-length fusion protein may not be normally produced in yeast system. It is known that the SBP domain of the SPL family members binds to the GTAC motif (Birkenbihl et al., 2005). Gel electrophoretic mobility shift assays (EMSAs) were performed to investigate whether OsSPL3 binds directly with GTAC motifs. OsSPL3 was able to bind the GTAC motif, but not the mutated motif GTGC (Figure 5C). Thus, OsSPL3 is a functional transcription factor with both transcription activation activity and DNA binding activity.

OsSPL12, but Not OsSPL4, Is Also a Regulator of Crown Root Development

Among the SPLs, OsSPL3, OsSPL4, and OsSPL12 were grouped into the same subclade, in which OsSPL12 had the highest level of amino acid sequence similarity to OsSPL3 in rice (Xie et al., 2006). RLM-RACE results indicated that *OsSPL4* and *OsSPL12* could be precisely cleaved by OsmiR156 in vivo (Figures 6A and 6B). To test whether OsSPL4 and OsSPL12 were also involved in crown root development, we produced *ProSPL4*:*smSPL4* and *ProSPL12*:*smSPL12* constructs with synonymous mutations in the OsmiR156-target site and transformed them into HJ2, respectively. *ProSPL12*:*smSPL12* transgenic plants showed decreased crown root numbers, like *lcrn1*, and highly elevated levels of *OsSPL12* transcripts in the basal nodes (Figures 6C and 6E). However, the *ProSPL4*:*smSPL4* transgenic plants did not show any defects in crown root development, despite the strongly elevated accumulation of *OsSPL4* transcripts (Figures 6C and 6D).

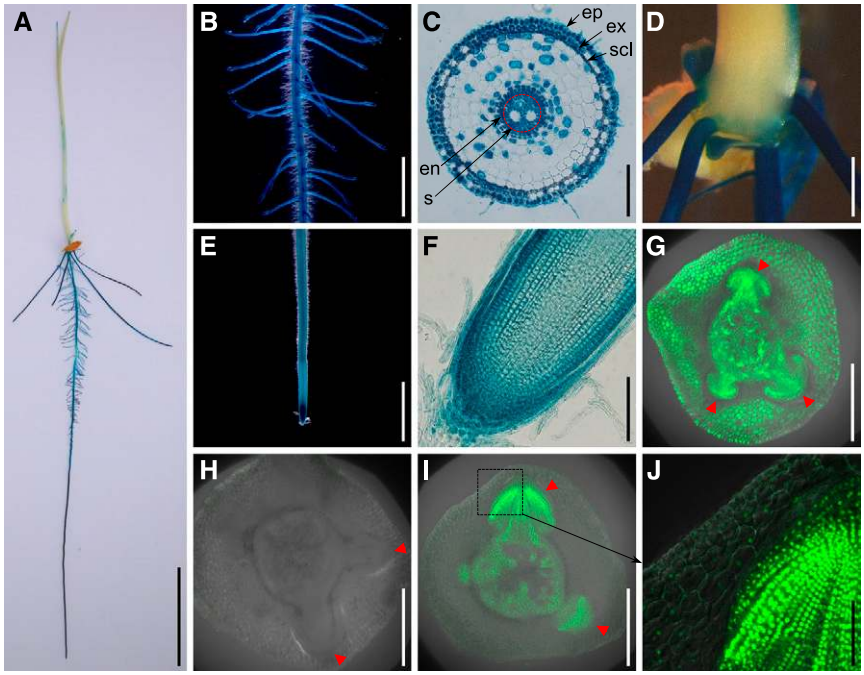

Figure 4. Tissue Expression Pattern of *OsSPL3* and Localization of OsSPL3 Protein in Crown Root Primordium.

(A) to **(F)** GUS staining of 5-d-old *ProSPL3*:*GUS* transgenic seedlings. **(A)** Whole seedling. **(B)** Primary root with lateral roots. **(C)** Cross section of the primary root maturation zone. **(D)** Stem base. **(E)** Root tip. **(F)** Longitudinal section of the root tip. Bars = 3 cm in **(A)**, 2 mm in **(B)** and **(E)**, 100 μm in **(C)** and **(F)**, and 1 mm in **(D)**.
(G) GFP fluorescence in the crown root primordia of the *ProSPL3*:*GFP* transgenic line. Bar = 500 μm.
(H) GFP fluorescence in the crown root primordia of the *ProSPL3*:*SPL3-GFP* transgenic line. Bar = 500 μm.
(I) GFP fluorescence in the crown root primordia of the *ProSPL3*:*smSPL3-GFP* transgenic line. Bar = 500 μm.
(J) Magnification of the box indicated in **(I)**. Bar = 100 μm.
Red arrowheads in **(G)** to **(I)** indicate crown root primordia. Abbreviations in **(C)**: en, endodermis; ep, epidermis; ex, exodermis; scl, sclerenchyma; s, stele.

Alternatively, clustered regularly interspaced short palindromic repeats (CRISPR)/ CRISPR associated protein 9 (Cas9)-generated *OsSPL3* single mutant (*spl3-crispr*) did not show any defects in crown root development compared with the wild type (Supplemental Figure 9). This result implies function redundancy among SPL proteins.

Genome-Wide Identification of OsSPL3-Target Genes

To identify the DNA binding sites and the target genes of OsSPL3 in rice, we performed a ChIP-seq analysis using the *ProSPL3*:*smSPL3-FLAG* transgenic lines, which contain synonymous mutations in the OsmiR156-target site. The phenotype of the *ProSPL3*:*smSPL3-FLAG* transgenic plants was similar to that of *lcrn1*, suggesting that the SPL3-FLAG fusion protein was functionally identical to OsSPL3 (Supplemental Figure 10). Five-day-old *ProSPL3*:*smSPL3-FLAG* transgenic plants were then used for the ChIP-seq analysis, with the wild-type plants as the negative control. Based on data from three biological repeats, 357 OsSPL3 binding sites were identified and grouped into 336 genes, which were referred to as OsSPL3-target genes (Supplemental Figure 11A; Supplemental Data Set 1). Of the 357 binding sites, 57.7% (206) were subsequently assigned to genic regions, located between –3000 bp of the transcription start site (TSS) and the end of the 3′ untranslated region (UTR; including the promoter, introns, exons, and 3′ UTR; Figure 7A). We then tested 10 randomly selected loci using ChIP-qPCR and verified the ChIP-seq data (Supplemental Figure 11B).

Further analysis revealed that more than 54% of the OsSPL3 binding sites occurred in promoter regions (the 3-kb sequence upstream of the TSS; Figure 7A). The histogram of the binding sites at the ±1-kb region around the TSSs revealed that the OsSPL3 binding sites were strongly enriched in the promoter region, peaking ~150 bp upstream of the TSSs, while the density of OsSPL3 binding sites was much lower in the gene-coding regions (Figure 7A; Supplemental Figure 11C). We next searched for significantly enriched motifs in the OsSPL3 binding sites using the Multiple EM for Motif Elicitation-ChIP program (Machanick and Bailey, 2011), and the OsSPL3 binding motif [GTAC(G/T)(A/G/T)] (P-value = $1.8e^{-108}$) was identified (Supplemental Figure 11D). A gene ontology (GO) analysis of the identified OsSPL3-target genes indicated that they were enriched in GO terms related to RNA biosynthetic processes, DNA binding, nucleic acid binding, and regulation of nucleic acid–templated transcription, implying that OsSPL3 could regulate different biological processes that affect plant growth and development (Supplemental Figure 11E).

To identify potential OsSPL3-target genes involved in crown root development, the transcriptional profiles of the basal nodes

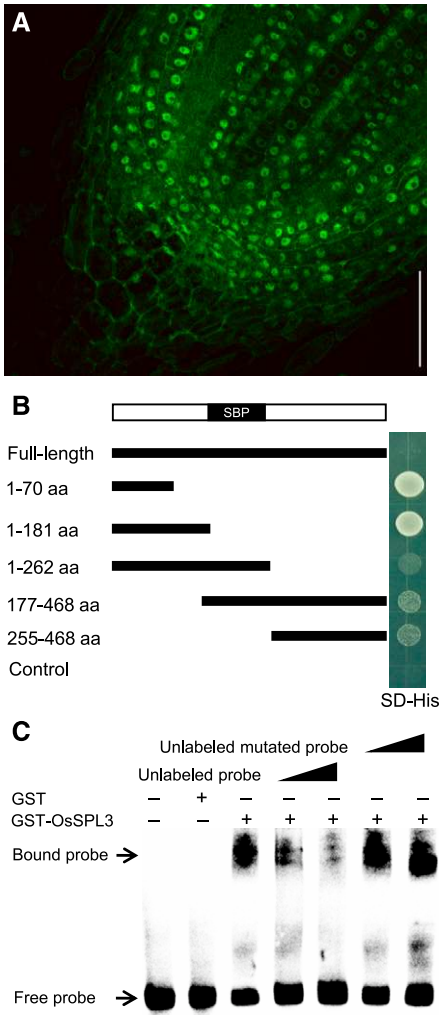

Figure 5. OsSPL3 Functions as a Transcription Factor.

(A) Subcellular localization of OsSPL3-GFP in rice root meristem cells. Bar = 50 μm.

(B) Yeast cells expressing the N terminus of OsSPL3 significantly promoted the growth of yeast cell on selective media. Yeast cells transformed with full-length and various truncated versions of OsSPL3 fused to the GAL4 binding domain were grown on selective media (SD−His). Empty vector was used as a negative control. aa, amino acids; SBP, SBP domain; SD, synthetically defined.

(C) OsSPL3 directly binds to the core sequence in a GTAC-dependent manner. A 63-bp probe containing the GTAC motifs was incubated with GST-OsSPL3 as indicated. Competition for OsSPL3 binding was performed with unlabeled or unlabeled mutated (GTGC) probe at 50 times and 150 times the amount of the labeled probe.

of the *lcrn1* and the wild-type plants were investigated using RNA-seq. For each genotype, the expression profiles of the three biological replicates were highly correlated with each other (Supplemental Figure 12A), indicating that our RNA-seq data were highly reproducible. In total, 1620 differentially expressed genes were found in the basal nodes [absolute value of $\log_2$ (ratio) ≥ 1, P-value < 0.05; Supplemental Data Set 2]. Among these differentially expressed genes, 1225 were downregulated and 395 were upregulated in *lcrn1* compared with the wild type (Figure 7B). The GO terms of these differently expressed genes, suggested that OsSPL3 could regulate several biological pathways that influence growth and development (Supplemental Figures 12B and 12C).

Combining the results from the ChIP-seq and RNA-seq analyses, 18 OsSPL3-target genes were determined to be putatively directly bound and transcriptionally regulated by OsSPL3 in the basal node where the crown root initiated (Figure 7C; Supplemental Data Set 3). Of these candidates, nine genes were downregulated and nine genes were upregulated in *lcrn1* (Figure 7C). Enriched GO terms of the genes were related to the nucleic acid binding transcription factor activity, regulation of nitrogen compound metabolic process, and regulation of RNA biosynthetic process. Furthermore, the molecular function ascribed to several target genes was transcription factor activity and

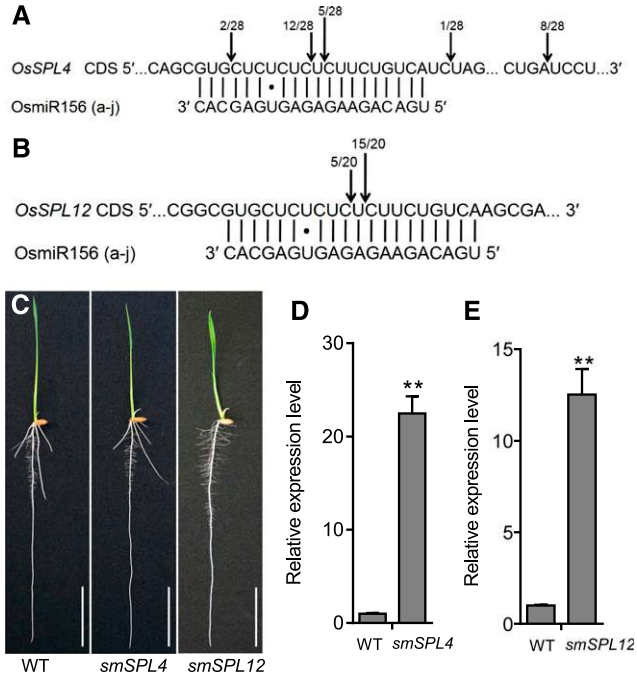

Figure 6. OsmiR156-Regulated *OsSPL12*, but not *OsSPL4*, Inhibits Crown Root Development in Rice.

(A) and **(B)** OsmiR156-mediated cleavage sites in *OsSPL4* **(A)** and *OsSPL12* **(B)** mRNAs determined using RLM-RACE. The vertical lines represent the nucleotides that base pair with OsmiR156, and dots show the mismatched nucleotides. The positions corresponding to the 5′ ends of the cleaved *OsSPL4* and *OsSPL12* mRNAs determined using 5′ RACE are indicated by arrows, and the number of 5′ RACE clones corresponding to each site are shown.

(C) Phenotypes of 5-d-old *ProSPL4:smSPL4* (*smSPL4*) and *ProSPL12:smSPL12* (*smSPL12*) transgenic plants. Bars = 3 cm. WT, wild type.

(D) and **(E)** Quantitative real-time PCR analysis of the expression of *OsSPL4* **(D)** and *OsSPL12* **(E)** in 5-d-old transgenic plants. Data were normalized to those of the wild type ([WT]; the level of WT was set to 1). Values are means + SD ($n = 3$ independent pools of basal nodes, five plants per pool). **Significant difference compared with WT (P < 0.01; Student's *t* test).

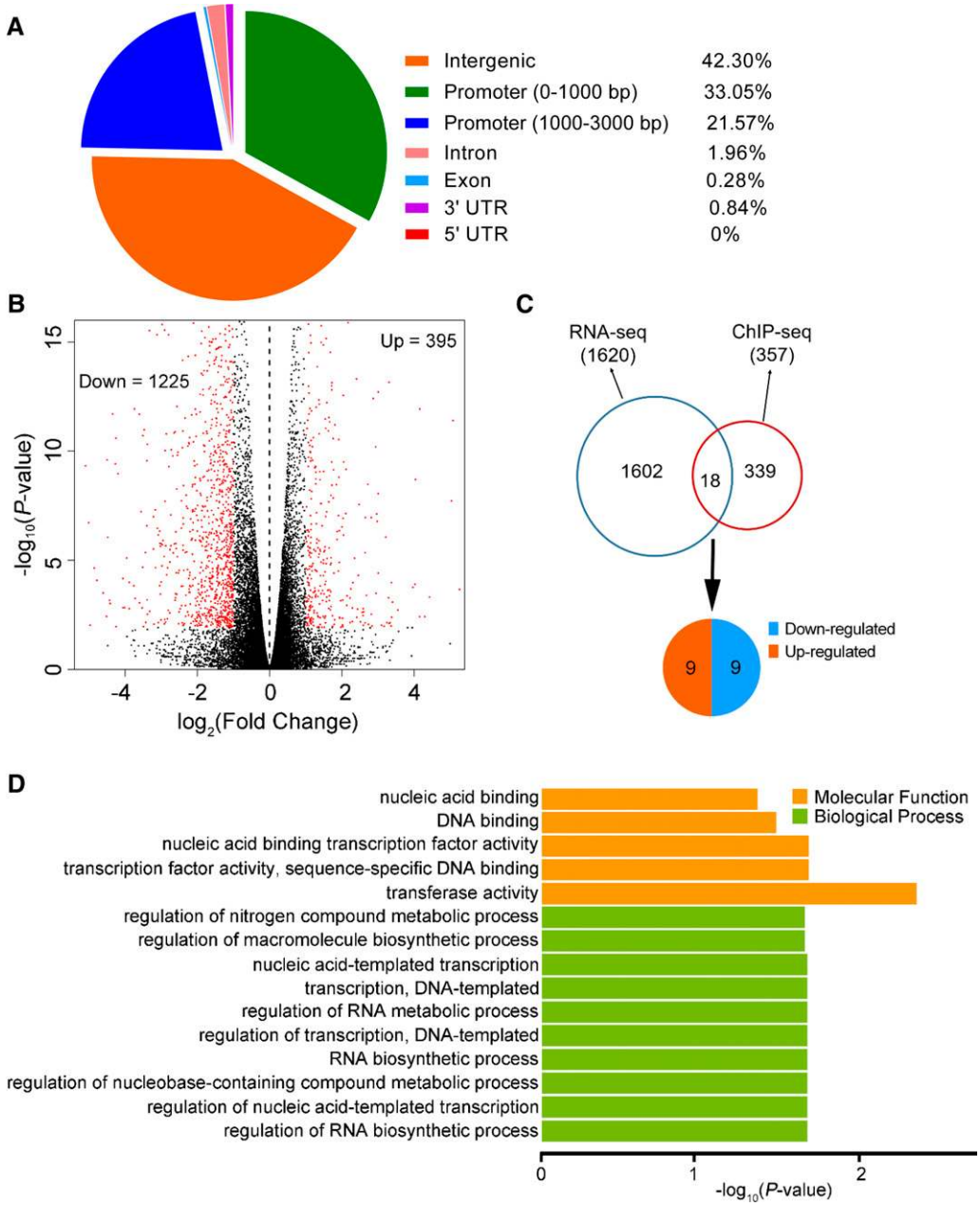

Figure 7. Genome-Wide Identification of OsSPL3 Binding Sites and Target Genes.

(A) Distribution of OsSPL3 binding sites in the rice genome.
(B) Volcano plot of differentially expressed genes between wild-type and *Icrn1* plants, revealed using RNA-seq. Down, downregulated genes, represented by red dots on the left; Up, upregulated genes, represented by red dots on the right.
(C) Identification of OsSPL3-target genes by combining OsSPL3 ChIP-seq data and RNA-seq data.
(D) Enrichment of GO terms among the 18 OsSPL3-target genes.

DNA binding (Figure 7D), suggesting that OsSPL3 may regulate crown root development by targeting other transcription factor(s).

OsSPL3 Positively Regulates *OsMADS50* Expression

AtSPLs are known to directly activate some MADS-box genes to regulate the switch from vegetative to reproductive development in Arabidopsis (Wang et al., 2009). *OsMADS50* was one of the 18 putative direct target genes of OsSPL3 identified and contains the potential OsSPL3 binding site. Quantitative real-time PCR analysis indicated that *OsMADS50* was expressed in root, basal node, elongated node, and flowers (Supplemental Figure 13A), which is consistent with that of *OsSPL3* (Figure 2C). The temporal expression patterns of *OsSPL3* and other *OsSPLs* are the opposite

of that of OsmiR156, with low expression levels in the seedling stage and high expression levels in the heading stage (Supplemental Figures 13B and 13C). Meanwhile, *OsMADS50* showed low expression level in the seedling stage and high expression level in the heading stage, which is consistent with that of *OsSPLs* (Supplemental Figure 13C). These results indicate that the spatial and temporal expression patterns of *OsMADS50* are overlapped with that of *OsSPL3*. Furthermore, the promoter of *OsMADS50* showed the highest enrichment of OsSPL3 among the target genes (Supplemental Data Set 3). Therefore, we hypothesized that *OsMADS50* is a direct target of OsSPL3 during crown root development. To test whether OsSPL3 can directly bind to the *OsMADS50* promoter, we performed an EMSA and revealed that glutathione S-transferase (GST)-SPL3 could bind to a 64-bp probe from the *OsMADS50* promoter containing the GTAC motif (Figure 8A). We further used a transient expression assay to analyze the effect of OsSPL3 on the expression of the firefly luciferase gene (*LUC*) driven by the *OsMADS50* promoter. Coexpression of *Pro35S*:*OsSPL3* with the *ProMADS50*:*LUC* construct led to an significant increase in luciferase activity compared with the vector control (Figure 8B), indicating that OsSPL3 functions as a transcriptional activator to upregulate the

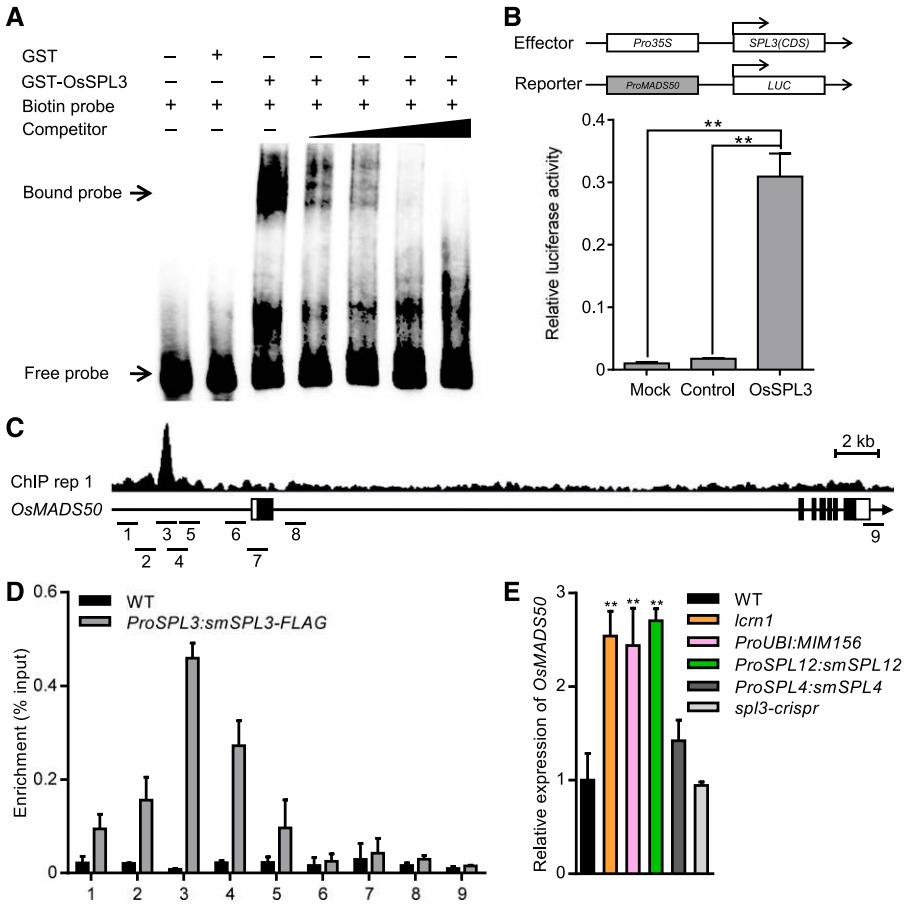

Figure 8. OsSPL3 Positively Regulates *OsMADS50* Expression.

(A) Results of an EMSA. Competition for OsSPL3 binding was performed with a cold probe (competitor) at 25 times, 50 times, 100 times, and 500 times the amount of the labeled probe (the promoter of *OsMADS50*, containing the GTAC motif).

(B) OsSPL3 activates the transcription of *OsMADS50*. Relative luciferase activity was monitored in tobacco leaves cotransfected with effector and reporter constructs. Mock, cotransfected with a reporter construct and an empty effector construct; control, cotransfected with an effector construct and an empty reporter construct. Values are means + SD (n = 3). **Significant difference ($P < 0.01$; Student's t test).

(C) Representative SPL3-FLAG ChIP-seq peaks (ChIP replicate 1) at *OsMADS50* revealed in Integrative Genomics Viewer. SPL3-FLAG peaks, gene structure, and the regions examined by ChIP-qPCR are shown in the top, middle, and bottom rows, respectively. The sequence regions marked 1 to 9 indicate the nine regions examined in the ChIP-qPCR assays. The black boxes represent exons and the lines between them represent introns, while the white boxes indicate untranslated regions. IGV, Integrative Genomics Viewer.

(D) Results of ChIP-qPCR assays using 5-d-old seedlings carrying the *ProSPL3*:*smSPL3-FLAG* transgene. Numbers 1 to 9 refer to the regions indicated in **(C)**. Primers are listed in Supplemental Data Set 4. Values are means + SD (n = 3 independent pools of seedlings). WT, wild type.

(E) Transcript levels of *OsMADS50* in the basal nodes of 3-d-old seedlings, as determined by quantitative real-time PCR. Data were normalized to those of the wild-type (WT) plants (the transcript level of WT was set to 1). Values are means + SD (n = 3 independent pools of basal nodes, five plants per pool). **Significant difference compared with WT ($P < 0.01$; Student's t test).

expression of *OsMADS50*. ChIP-seq data showed that SPL3-FLAG binding peaks were located at the promoter region of *OsMADS50* (Figure 8C). Consistently, ChIP-qPCR analysis of *ProSPL3*:*smSPL3-FLAG* transgenic lines similarly revealed the occupancy of OsSPL3 at the 5′ promoter region, demonstrating direct association of OsSPL3 with the promoter of *OsMADS50* (Figures 8C and 8D).

A quantitative real-time PCR analysis confirmed that the transcript level of *OsMADS50* was upregulated in the basal node of the *lcrn1* mutants compared with the wild type (Figure 8E). Moreover, the transcript abundance of *OsMADS50* was increased in the basal node of the OsmiR156-target mimic transgenic line *ProUBI*:*MIM156*, which had elevated expression levels of the *SPL* genes (Figure 8E). The transcript level of *OsMADS50* was also upregulated in the basal node of *ProSPL12*:*smSPL12* transgenic plants, but only slightly increased in *ProSPL4*:*smSPL4* transgenic plants (Figure 8E). The transcript level of *OsMADS50* was not changed in the OsSPL3 loss-of-function mutant (*spl3-crispr*), consistent with its comparable phenotype with the wild type (Figure 8E; Supplemental Figure 9).

Taken together, these results show that *OsMADS50* is a direct target of OsSPL3 and is positively regulated by both OsSPL3 and OsSPL12 in rice nodes.

OsMADS50 Mediates *OsSPL3* Function in Crown Root Development

To investigate whether *OsMADS50* is involved in crown root development, *OsMADS50*-overexpressing transgenic plants were generated. At 5 DAG, the *OsMAS50*-overexpressing seedlings had no crown roots (Figures 9A and 9C), while at 39 DAG they had produced substantially fewer crown roots than the wild-type plants, phenocopying *lcrn1* (Figures 9B and 9D). The crown root number, plant height, and tiller numbers at different growth stages were also measured, revealing that the *OsMADS50*-overexpressing lines had fewer crown roots, shorter heights, and fewer tillers than the wild type (Figure 9E; Supplemental Figure 14). The *OsMADS50*-overexpressing line produced slightly more crown roots than *lcrn1* before 19 DAG, but significantly fewer crown roots than *lcrn1* after 33 days of growth (Figure 9E).

To investigate the genetic interaction between *OsSPL3* and *OsMADS50*, we generated a *lcrn1 mads50* double mutant by introducing a mutation in *OsMADS50* in the *lcrn1* background using CRISPR/Cas9 technology. A sequence analysis revealed the presence of a G deletion at the fourth base and a 22-bp deletion between bases 133 to 154 of the *OsMADS50* CDS in the *lcrn1 mads50-2* double mutant, which resulted in a frameshift and a truncated OsMADS50 protein (Supplemental Figures 15A to 15C). A phenotypic analysis showed that while the 5 DAG *lcrn1* mutants did not form any crown roots, the *lcrn1 mads50-2* double mutant formed one crown root (Figures 9A and 9C). Compared with the *lcrn1* lines, the double mutant line had more crown roots at each developmental stage, especially after 19 DAG, but it produced fewer crown roots than the wild type (Figures 9B, 9D, and 9E). At 33 DAG, *lcrn1* had ~33 roots and *lcrn1 mads50* had ~57 roots, while the wild-type plants had formed 88 roots (Figure 9E). After 47 d, *lcrn1* had produced ~60 roots, *lcrn1 mads50* had ~104 roots, and the wild-type plants had formed 130 roots (Figure 9E).

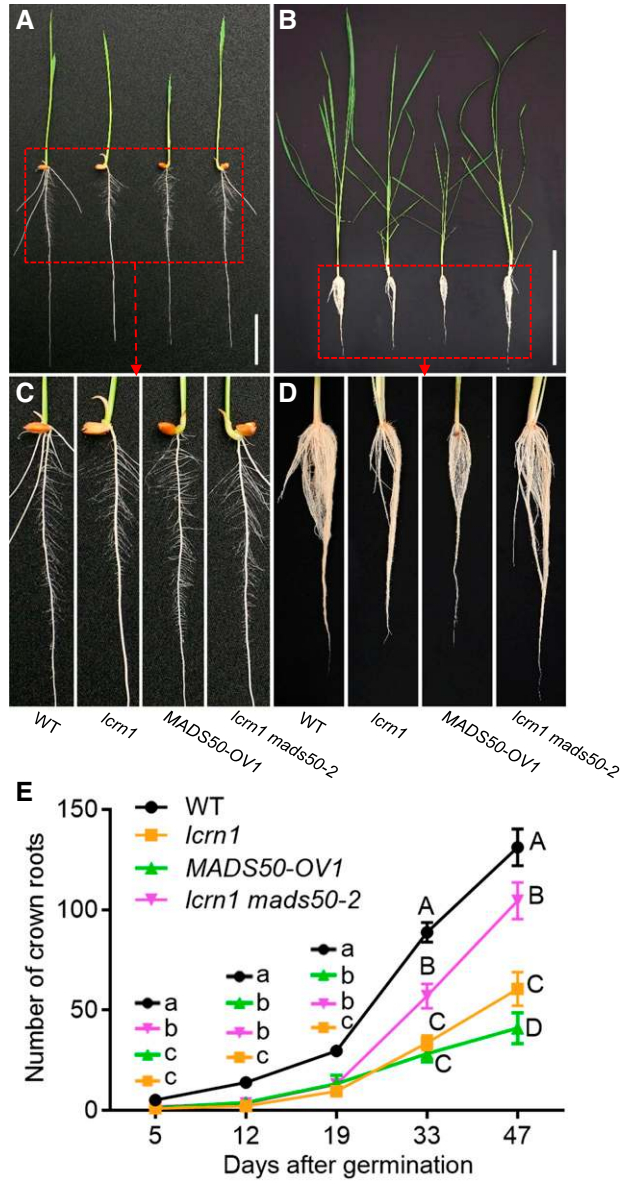

Figure 9. Phenotypes of Wild-Type, *lcrn1*, *MADS50*-Overexpressing Transgenic Line, and *lcrn1 mads50* Double Mutant Plants.

(A) Phenotypes of 5-d-old wild-type, *lcrn1*, the *MADS50*-overexpressing transgenic line (*MADS50-OV1*), and *lcrn1 mads50-2* double mutant plants. Bar = 3 cm.

(B) Phenotypes of 39-d-old plants. Bar = 40 cm.

(C) and **(D)** Magnified view of the boxed area in **(A)** and **(B)**.

(E) Number of crown roots at different growth stages. Data are shown as means ± SD (n = 20 independent plants). Significantly different values are indicated by different letters (lowercase letters, $P < 0.05$; uppercase letters, $P < 0.01$; one-way ANOVA with Tukey's honestly significant difference test). WT, wild type.

These results indicated that the *mads50* mutation could partially recover the reduced crown root phenotype of *lcrn1*.

To further investigate the biological function of *OsMADS50*, we crossed the *lcrn1 mads50* double mutant with HJ2 to obtain the

mads50 single mutant in the HJ2 background (Supplemental Figure 16). Crown root development in the *mads50* plants was similar to the wild type at the young seedling stage (Supplemental Figure 16A) and at the later stages of development (Supplemental Figure 16B). The numbers of crown roots in *mads50* were not significantly different to the wild-type plants (Supplemental Figure 16D).

Taken together, these results indicate that *OsSPL3* inhibits crown root development through positive regulation of *OsMADS50*.

The *OsSPL3-OsMADS50* Module Affects Auxin Signaling

RNA-seq analyses indicated that the expression of a series of auxin signaling–related genes were significantly altered in *lcrn1* compared with the wild type (Supplemental Data Set 2). This result suggests that the *OsSPL3-OsMADS50* module may regulate auxin transport and signaling components to regulate crown root development. To investigate whether the *OsSPL3-OsMADS50* module regulates auxin transport and signaling, we analyzed the expression levels of auxin signaling–related genes in the basal node of *lcrn1* and *OsMADS50*-overexpressing transgenic lines.

ARL1/*CRL1* and *CRL4*, two auxin signaling–related genes, are important regulators of crown root development in rice (Inukai et al., 2005; Liu et al., 2005, 2009; Kitomi et al., 2008). Quantitative real-time PCR results showed that the transcript level of *ARL1*/*CRL1* was slightly downregulated in *lcrn1* and *OsMADS50*-overexpressing transgenic lines compared with that in the wild type (Figure 10). In this study, we isolated a weak *arl1* mutant, which can form three to five crown roots (Supplemental Figure 17); however, the *lcrn1 arl1* double mutant did not produce any crown roots during the growth period, a phenotype more severe than that of the *lcrn1* or *arl1* single mutants (Supplemental Figure 17). This result suggests that *OsSPL3* did not target *ARL1* to regulate crown root development. Furthermore, the expression level of *CRL4* was not significantly affected in the *lcrn1* and *OsMADS50*-overexpressing transgenic lines (Figure 10).

OsIAA23 is reported to regulate crown root development (Jun et al., 2011). To analyze whether the *OsSPL3-OsMADS50* module affects the expression of auxin-responsive *Auxin/IAA* genes, eight *OsIAA* genes with relatively large changes in *lcrn1* compared with the wild type in the RNA-seq data were analyzed by quantitative real-time PCR (Figure 10). The expression levels of most *OsIAA* genes (*OsIAA4*, *OsIAA7, OsIAA9, OsIAA11*, *OsIAA13*, *OsIAA23*, and *OsIAA31*) were relatively repressed in the basal node of *lcrn1*, but not in *OsMADS50*-overexpressing transgenic lines, except for *OsIAA5*, which was significantly repressed in both *lcrn1* and *OsMADS50*-overexpressing transgenic lines (Figure 10).

OsARF genes play a key role in regulating the expression of early auxin-responsive genes. To analyze whether the *OsSPL3-OsMADS50* module regulates *OsARF* genes, five *OsARF* genes with relatively large changes in *lcrn1* compared with the wild type in the RNA-seq data were further analyzed by quantitative

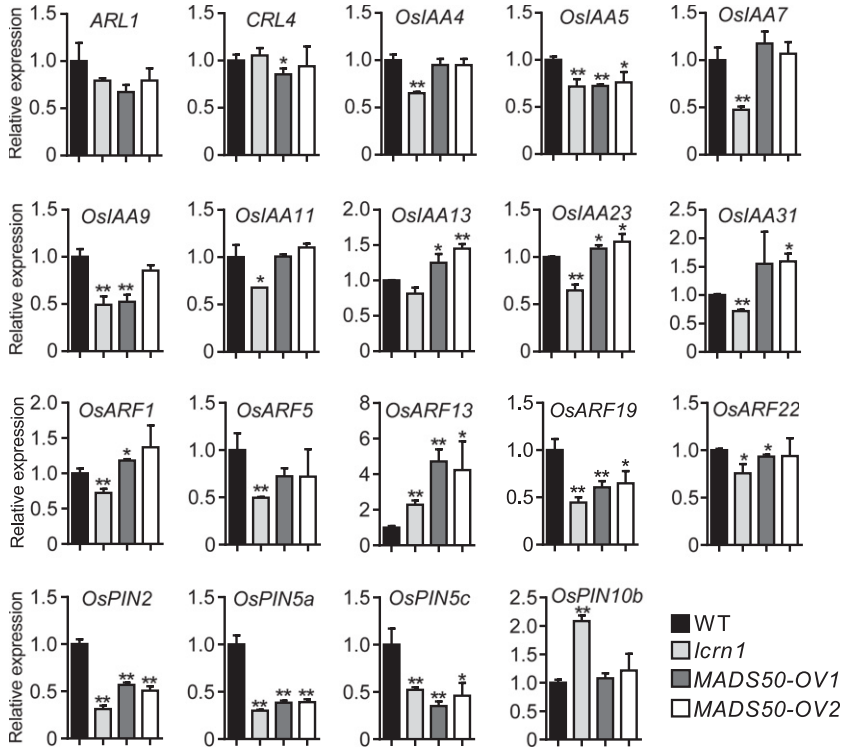

Figure 10. Expression of Auxin Signaling–Related Genes in Basal Nodes of Wild-Type, *lcrn1*, and *OsMADS50*-Overexpressing Transgenic Plants.

Relative expression levels of auxin signaling–related genes were analyzed in basal nodes of the 3-d-old wild-type (WT), *lcrn1*, and two independent *OsMADS50*-overexpressing transgenic lines. *ACTIN1* was used as an internal control. Transcript level of the WT was set at 1. Values are means + SD ($n = 3$ independent pools of basal nodes, five plants per pool). Significant difference compared with WT (*P < 0.05; **P < 0.01; Student's *t* test).

real-time PCR. The expression of *OsARF1*, *OsARF5*, and *OsARF22* were significantly repressed in *lcrn1*, but not in *OsMADS50*-overexpressing transgenic lines, while the expression of *OsARF19* was significantly repressed in *lcrn1* and *OsMADS50*-overexpressing transgenic lines compared with that in the wild type (Figure 10). However, *OsARF13* is upregulated in *lcrn1* and *OsMADS50*-overexpressing transgenic lines compared with that in the wild type (Figure 10).

Four *OsPIN* genes (*OsPIN2*, *OsPIN5a*, *OsPIN5c*, and *OsPIN10b*) that had significantly altered expression in *lcrn1* compared with the wild type in RNA-seq data [absolute value of $\log_2$ (ratio) ≥ 1, P-value < 0.05; Supplemental Data Set 2] were further investigated using quantitative real-time PCR. Expression of *OsPIN2*, *OsPIN5a*, and *OsPIN5c* was highly repressed in *lcrn1* and *OsMADS50*-overexpressing transgenic lines, while *OsPIN10b* was induced in *lcrn1*, but not in *OsMADS50*-overexpressing transgenic lines (Figure 10). These results suggested that *OsSPL3-OsMADS50* might be directly or indirectly involved in regulating *OsPIN2*, *OsPIN5a*, and *OsPIN5c*.

To investigate whether *OsSPL3* and *OsMADS50* were responsive to auxin and cytokinin, 6-d-old seedlings were treated with IAA, NAA, and 6-benzylaminopurine (6-BA) for different times. The expression of *OsSPL3* or *OsMADS50* in stem bases harvested at different time points was tested by quantitative real-time PCR. *OsSPL3* or *OsMADS50* expression was not very responsive to IAA, NAA, or 6-BA treatment (Supplemental Figures 18A and 18B). We also analyzed the content of auxin and cytokinin in the wild-type, *lcrn1*, and two *OsMADS50*-overexpressing transgenic seedlings. The content of IAA, *cis*-zeatin riboside, *cis*-zeatin, isopentenyladenine, and dihydrozeatin was not significantly different among these plants (Supplemental Figure 18C). These observations indicate that *OsSPL3* and *OsMADS50* do not affect the biosynthesis or metabolism of auxin and cytokinin.

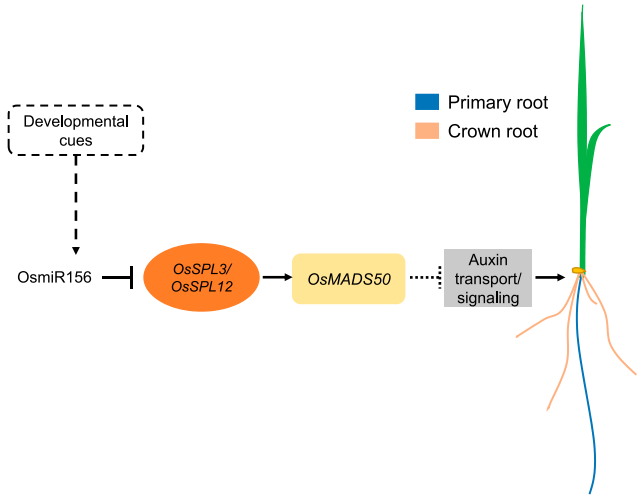

Figure 11. A Working Model for the *OsSPL3*-Mediated Regulation of Crown Root Development.

In basal nodes of seedlings, high levels of OsmiR156 cleave *OsSPL3* and *OsSPL12* transcripts and thereby repress the expression of *OsMADS50* (OsSPL3 and OsSPL12 positively regulate the expression level of *OsMADS50*). OsMADS50 may negatively regulate auxin transport and signaling, which are essential for crown root development. Positive and negative regulatory effects are indicated by arrows and flat-ended lines, respectively. Dashed lines indicate interactions that have not been experimentally confirmed.

DISCUSSION

In this study, we elucidated a novel molecular pathway in which the OsmiR156-*OsSPL3*/*OsSPL12* module directly activates *OsMADS50* activity in the node to regulate crown root development in rice (Figure 11). In basal nodes, where the crown roots are initiated, the OsmiR156-mediated degradation of the *OsSPL3* and *OsSPL12* transcripts decreases the amount of OsSPL3/OsSPL12 and the expression of its target gene *OsMADS50*, enabling the crown roots to develop (Figure 8E; Supplemental Figure 5A). In the *lcrn1* mutant, OsmiR156 cannot target the mutated *OsSPL3* transcripts, resulting in high levels of OsSPL3 and the upregulated expression of *OsMADS50*, which consequently suppresses crown root development (Figure 8E; Supplemental Figure 6).

OsmiR156-*OsSPL3*-*OsMADS50* Is a Novel Molecular Pathway Regulating Crown Root Development

In this study, we identified an *SPL* gene that functions in root development in cereals. *OsSPL3* serves as a negative regulator of crown root development. Our results indicated that a single nucleotide substitution in *OsSPL3* perturbed the cleavage of the *OsSPL3* transcripts targeted by OsmiR156, which led to the accumulation of *OsSPL3* transcripts in *lcrn1* (Figures 2B and 2C; Supplemental Figure 6). The accumulation of *OsSPL3* then restricted crown root development throughout the growth period (Figures 1A and 1B). The GFP fluorescence observed in the *ProSPL3*:*GFP* transgenic line indicated that *OsSPL3* is highly expressed in crown root primordia and the peripheral cylinder of the vascular bundles (Figure 4G). GFP fluorescence was also detected in these tissues in the *ProSPL3*:*smSPL3-GFP* transgenic line (Figure 4I); however, no GFP fluorescence was detected in the *ProSPL3*:*SPL3-GFP* transgenic line (Figure 4H), suggesting that *OsSPL3* is posttranscriptionally suppressed in the basal nodes of young seedlings.

The *ProSPL12*:*smSPL12* transgenic plants produce fewer crown roots than the wild type, phenocopying *lcrn1* (Figure 6C), suggesting that there might be functional overlap among members of the *OsSPL* family genes. The *ProSPL4*:*smSPL4* transgenic plants did not have any defects in their crown root development, despite their highly increased accumulation of *OsSPL4* transcripts (Figures 6C and 6D). These results suggest that OsSPL3 and OsSPL12, but not OsSPL4, are specifically involved in regulating crown root development. The *spl3-crispr* loss-of-function mutants did not show any defects in crown root development, suggesting a functional redundancy between *OsSPL3* and *OsSPL12* or even other *OsSPLs* (Figures 6C; Supplemental Figure 9).

Furthermore, our results showed that *OsMADS50* was a direct target of OsSPL3, which positively regulated its expression (Figures 8 and 9). To date, the MADS-box transcription factors have mainly been known as regulators involved in floral organ specification and the switch from vegetative-to-reproductive

development in cereals and Arabidopsis (Arora et al., 2007; Yan et al., 2016). MADS-box transcription factors were also found to play important roles in root development (Garay-Arroyo et al., 2013; Yu et al., 2014, 2015; Gao et al., 2018; Sun et al., 2018). However, to date, no MADS-box genes has been reported to function in crown root development in cereals. The overexpression of *OsMADS50* resulted in the suppression of crown root development, which phenocopied *lcrn1* throughout crown root development (Figure 9). We therefore conclude that OsMADS50 is a newly identified negative regulator of crown root development in cereals.

Compared with *lcrn1*, the number of crown roots in the *lcrn1 mads50* double mutants were significantly increased; however, they did not produce as many crown roots as the wild-type plants (Figures 9B, 9D, and 9E). These results suggest that *OsSPL3* may also activate other MADS-box genes to inhibit the initiation of crown root development. The crown root development of the *mads50* mutant did not differ from that of the wild type (Supplemental Figure 16), suggesting a functional redundancy among the MADS proteins. There are 75 MADS-box genes in rice (Arora et al., 2007). The results of our ChIP-seq analysis indicated that OsSPL3 also binds to the promoter of *OsMADS56*, a member of the TM3-like MADS-box genes as *OsMADS50* (Supplemental Data Set 1); however, no induction of *OsMADS56* was detected in the RNA-seq data from *lcrn1*. It is possible that the expression level of *OsMADS56* was too low to be detected in the RNA-seq analyses. Further studies are required to determine whether other MADS proteins are involved in crown root development in rice. We also identified many other genes that are potential direct targets of OsSPL3 (Supplemental Data Set 3), and their putative roles in crown root development also require further elucidation.

Altogether, our data suggest that OsmiR156-*OsSPL3*/*OsSPL12*-*OsMADS50* is a novel molecular pathway that regulates crown root development.

OsSPL3-*OsMADS50* Regulates Auxin Signaling–Related Genes

In addition to the defect in crown root formation, *lcrn1* showed impaired root gravitropism (Supplemental Figures 1C and 1D), was less sensitive to auxin treatment in crown root formation (Supplemental Table), and had a decreased lateral root number (Supplemental Figure 2C). These results suggested that *OsSPL3*-*OsMADS50* might regulate crown root development by affecting auxin signaling. Our data showed that *OsSPL3* or *OsMADS50* was not very responsive to auxin and cytokinin treatment ((Supplemental Figures 18A and 18B). However, overexpression of *OsSPL3* or *OsMADS50* either activated or repressed the expression of some auxin signaling–related genes (e.g., *OsIAA5*, *OsARF13*, and *OsARF19*; Figure 10). Quantitative real-time PCR analysis showed that *OsPIN2*, *OsPIN5a*, and *OsPIN5c*, which are thought to be auxin transporters (Xu et al., 2005; Wang et al., 2018a), were highly repressed by overexpression of *OsSPL3* and *OsMADS50* (Figure 10). It is reported in Arabidopsis that the MADS transcription factor XAANTAL2 modulates auxin transport during root development by directly regulating *PIN* expression (Garay-Arroyo et al., 2013). Recently, the MADS transcription factor chrysanthemum homolog of the Arabidopsis protein AtANR1 was reported to modulates chrysanthemum adventitious root and lateral root development by directly regulating *CmPIN2* expression (Sun et al., 2018). These results suggest that the *OsSPL3*-*OsMADS50* module might be directly involved in regulating *OsPIN2*, *OsPIN5a*, and *OsPIN5c* expression to modulate crown root development.

The RRs are thought to be important integration points for CK signaling in the regulation of crown root development (Zhao et al., 2009, 2015); however, no *RR* genes were significantly up- or downregulated in *lcrn1* compared with the wild type (Supplemental Data Set 2). These results suggest that *OsSPL3* may not regulate CK signaling.

No significant differences in the content of auxin and CK in the *lcrn1* mutants and *OsMADS50*-overexpressing transgenic plants compared with the wild type (Supplemental Figure 18C), suggesting that *OsSPL3*-*OsMADS50* might not regulate the synthesis or metabolism of auxin and CK.

Thus, the *OsSPL3*-*OsMADS50* pathway may regulate the auxin transport and signaling pathway to influence crown root development; however, the direct downstream targets of *OsMADS50* have yet to be determined.

OsmiR156-*OsSPL3*-*OsMADS50* May Be Involved in Adventitious Rooting in Maturing Plants

The relative expression of miR156 and its target *SPLs* in the nodes of rice plants suggests they may be developmentally regulated. *OsSPL3* expression was low in the basal nodes in young seedlings but was high in the basal and upper nodes of plants at the heading stage. This pattern contrasts with the expression pattern of OsmiR156 in vivo (Supplemental Figures 5A, 13B, and 13C). Further results indicated that in the basal nodes of young rice seedlings, the OsmiR156 transcript levels are high, while the levels of *OsSPL3*, *OsSPL12*, and *OsMADS50* are low (Supplemental Figures 5A, 13B and 13C), but the crown (adventitious) rooting ability is high at this stage. At the heading stage, OsmiR156 levels gradually decline, with a concomitant rise in the transcript levels of *OsSPL3*, *OsSPL12*, and other *OsSPL* genes (Supplemental Figures 5A, 13B and 13C), causing the upregulation of *OsMADS50*, which inhibits adventitious rooting (Figure 8E; Supplemental Figure 13C). This suggests that the OsmiR156-*OsSPL3*-*OsMADS50* pathway might be a potential target for promoting the rooting ability of rice plants in the maturation stage; the expression levels of *OsSPL3* or *OsMADS50* could be repressed to prevent premature senescence in rice.

The MiR156-*SPL* Module Is Probably a Conserved Regulator of Adventitious Rooting in Plants

It is noteworthy that miR156 and *SPL* genes arose early in plant evolution and are present in all land plants examined to date (Klein et al., 1996; Axtell and Bartel, 2005), although their specific roles were obscure. In this study, we found that the OsmiR156-regulated *OsSPL3* and *OsSPL12* repress adventitious root development in rice (Figures 6C and 11). miR156 was reported to affect rooting in several species (Chuck et al., 2007; Zhang et al., 2011; Feng et al., 2016; Aung et al., 2017; Massoumi et al., 2017;

Xu et al., 2017). In maize (*Zea mays*), *corngrass1* mutants have elevated miR156 levels and produce more crown roots (Chuck et al., 2007). In dicots, adventitious root production is increased in tomato (*Solanum lycopersicum*) and tobacco (*Nicotiana tabacum*) plants with elevated levels of miR156 (Zhang et al., 2011; Feng et al., 2016). In the Chinese crab apple (*Malus baccata* var *xiaojinensis*), high miR156 expression levels promote adventitious root formation (Xu et al., 2017). Furthermore, *SPL*s have been reported to repress adventitious root development from the base of the hypocotyl when the root system of Arabidopsis seedlings is removed to induce root production (Xu et al., 2016). Furthermore, *SPL* expression is found to increase in the successive nodes of woody plants, which explains the association between shoot age and the loss of rooting capacity in these species (Basheer-Salimia, 2007; Wang et al., 2011a). These results imply that the miR156-*SPL* module may be conserved in regulating adventitious root production in all land plants.

In this study, we found that the OsmiR156-regulated *OsSPL3* and *OsSPL12* repress crown root development in rice mainly through the activity of transcription factor OsMADS50 downstream of the OsmiR156-*OsSPL3/OsSPL12* module (Figures 6C and 11). Whether MADS-box genes in other plants function as downstream targets of SPLs in the regulation of adventitious rooting awaits further investigation. Adventitious (crown) roots are of great agronomic importance for plant anchoring as well as water and nutrient uptake in cereals. Adventitious rooting is also required for the vegetative propagation of plants and the successful clonal multiplication of elite genotypes of forest, horticultural, and agricultural plant species. Our results contribute additional regulatory components to facilitate the improvement of the adventitious rooting ability of cereals and probably also perennial woody plants.

METHODS

Plant Materials and Growth Conditions

The EMS-mutated mutant library was generated using the *indica* rice cv Kasalath (Kas, as described previously in Jia et al. (2011), and then screened for mutants with abnormal crown root development. The *lcrn1*^{Kas} mutant was isolated and crossed with a *japonica* rice cultivar, Hei Jing2 (HJ2), with a shorter growth period. The F_1 plants were backcrossed eight times with HJ2 to generate the near-isogenic mutant line *lcrn1* in the HJ2 background. The *arl1* mutant line S2409 (named according to its original line number) was identified from a screen of an EMS-mutated mutant library in the *japonica* rice cv Shi Shou Bai Mao background. The phenotypic characterization of the wild-type and mutant plants was performed in a growth chamber at 30°C/22°C (day/night) and 60% to 70% humidity, bulb type light with a photon density of ~300 μmol m^{-2} s^{-1}, and a photoperiod of 14 h. For the hydroponically grown plants, the seedlings were grown in full-strength Kimura nutrient solution as described previously (Chen et al., 2013). *Nicotiana benthamiana* plants were cultivated in growth chambers, as described previously (Lv et al., 2014).

Map-Based Cloning

For the map-based cloning, *lcrn1*^{Kas} was crossed with HJ2 to create the F_2 population from which 30 plants with low crown root numbers were selected for primary mapping. *LCRN1* was first mapped onto chromosome 2 using simple sequence repeat markers and sequence-tagged-site markers and then further fine-mapped using 100 plants with mutant phenotypes. *LCRN1* was then cloned based on a genome resequencing using the MutMap method (Yang et al., 2016). DNA was extracted from Kas and *lcrn1*^{Kas}, and then the genome resequencing was performed with a mean coverage of 30 times using an Illumina HiSeq2500 sequencer. This analysis revealed 10 SNPs and eight indels between Kas and *lcrn1*^{Kas} in the mapping region, all but two of which occurred upstream or downstream of genic regions, in introns, or generated synonymous mutations. One SNP was located in LOC_Os02g04680.1 and one indel was located in LOC_Os02g05170.1. LOC_Os02g05170.1 is annotated as a retrotransposon protein; therefore, LOC_Os02g04680.1, which encodes OsSPL3, was selected as the candidate gene. A derived cleaved amplified polymorphic sequence marker was also developed to identify the *lcrn1* mutant (Figure 2D). All the primers used are listed in Supplemental Data Set 4.

Construction of Vectors and the Generation of Transgenic Plants

To verify *OsSPL3* as the gene responsible for the *lcrn1* phenotype, the *ProSPL3*:*mSPL3* allele was constructed in HJ2. An ~7.0-kb DNA fragment containing a 3196-bp sequence upstream of the start codon, the entire *OsSPL3* gene sequence, and a 488-bp sequence downstream of the stop codon was amplified from the HJ2 genomic DNA using PrimeSTAR (PrimeSTAR HS DNA polymerase, Takara). The point mutation in *OsSPL3* was introduced using an overlap extension PCR, and then the mutated *OsSPL3* gene was ligated into the binary vector pCAMBIA1300 for plant transformation.

To construct the *ProSPL3*:*smSPL3* vector, an ~7.0-kb DNA fragment containing a 3196-bp sequence upstream of the start codon, the entire *OsSPL3* gene sequence, and a 488-bp sequence downstream of the stop codon was amplified from HJ2 genomic DNA using PrimeSTAR, and the synonymous mutations of *OsSPL3* (*OssmSPL3*) in the OsmiR156-target site were introduced using overlap extension PCR. The mutated DNA was then ligated into the binary vector pCAMBIA1300 for plant transformation.

To generate the *ProSPL3*:*GUS* or *ProSPL3*:*GFP* constructs, the 3196-bp sequence upstream of the *OsSPL3* start codon was amplified from HJ2 genomic DNA using PrimeSTAR, and then fused with *GUS* or *GFP* in the modified pCAMBIA1300-GUS or pCAMBIA1300-sGFP vectors.

To construct the *ProSPL3*:*smSPL3-GFP* or *ProSPL3*:*smSPL3-FLAG* vectors, an ~6.5-kb DNA fragment containing genomic *OsSPL3* and the 3196-bp region upstream of the *OsSPL3* start codon was amplified from HJ2 genomic DNA using PrimeSTAR. The synonymous mutations of *OsSPL3* were introduced using overlap extension PCR and then fused in-frame to the 5′ end of sGFP or FLAG in the modified pCAMBIA1300-sGFP or pCAMBIA1300-FLAG vectors, respectively.

To construct the vector carrying *ProSPL4*:*smSPL4*, an ~7.2-kb DNA fragment containing the 2879-bp sequence upstream of the start codon, the entire *OsSPL4* gene sequence, and the 1221-bp sequence downstream of the stop codon were amplified from HJ2 genomic DNA using PrimeSTAR. The same synonymous mutations as used in *ProSPL3*:*smSPL3* were introduced to the OsmiR156-target site using overlap extension PCR, and then the DNA was ligated into the binary vector pCAMBIA1300 for plant transformation.

To generate the *ProSPL12*:*smSPL12* construct, an ~8.0-kb DNA fragment containing the 4126-bp sequence upstream of the start codon, the entire *OsSPL12* gene sequence, and the 631-bp sequence downstream of the stop codon were amplified from HJ2 genomic DNA using PrimeSTAR. The same synonymous mutations as used in *ProSPL3*:*smSPL3* were introduced into the OsmiR156-target site using overlap extension PCR and then ligated into the binary vector pCAMBIA1300 for plant transformation.

To make the *OsMADS50*-overexpressing vector *Pro35S*:*OsMADS50*, the 693-bp CDS of *OsMADS50* was amplified from HJ2 cDNA using PrimeSTAR and cloned into a binary overexpression vector, modified pCAMBIA1300, driven by the cauliflower mosaic virus 35S promoter.

To generate the *spl3* and *mads50* knockout mutants, two specific targets at different locations of *OsSPL3* and *OsMADS50*, respectively, were selected to generate the CRISPR/Cas9 vectors (Zhu et al., 2014). The sequences were ligated into the pYLCRISPR/gRNA vector, followed by a ligation into the pYLCRISPR/Cas9-MH vector as described previously in Zhu et al. (2014).

All the constructs were transformed into callus induced from mature embryos of HJ2 to generate transgenic plants via *Agrobacterium tumefaciens* strain EHA105–mediated transformation, as described previously (Wang et al., 2014). The primers used (including the restriction enzyme sites used in the cloning) are listed in Supplemental Data Set 4.

RNA Ligase–Mediated Rapid Amplification of cDNA Ends (RLM-RACE)

An RLM-RACE was performed according to the method described previously (Llave et al., 2002). Briefly, total RNA was isolated from 10-d-old HJ2 seedlings using TRIzol reagent (Thermo Fisher Scientific). Primers specific for *OsSPL3*, *OsSPL4*, and *OsSPL12* (listed in Supplemental Data Set 4) were used to amplify unique gene-specific DNA fragments. PCR products were gel purified and cloned into the T-vector pMD19 (Takara) using TA cloning method for sequencing.

RNA Isolation, RT-PCR, and Quantitative Real-Time PCR Analysis

Total RNA was isolated using TRIzol reagent (Thermo Fisher Scientific) or an RNeasy Plant Mini Kit (Qiagen), followed by a treatment with DNase I (Qiagen) before RT. cDNA was synthesized from 5 μg of total RNA using a RT kit (Promega). Quantitative real-time PCRs were performed using the FastStart Universal SYBR Green Master mix (Roche) on a LightCycler 480 Real-Time PCR system (Roche), according to the manufacturer's instructions. Relative expression levels were normalized to the internal control gene *OsACTIN1*.

The quantitative real-time PCR to quantify the amount of mature OsmiR156 was performed following a published protocol (Varkonyi-Gasic et al., 2007). Relative expression levels of OsmiR156 were normalized to the internal control miRNA U6. The primers used for the RT-PCR and quantitative real-time PCR analyses are listed in Supplemental Data Set 4.

ChIP-Seq Analysis

HJ2 and the *ProSPL3*:*smSPL3-FLAG* transgenic lines were used for the ChIP assays according to a method described previously (Lv et al., 2014), with some modifications. Briefly, 2 g of 5-d-old whole seedlings grown in hydroponic solution was harvested and then cross-linked with 1% (v/v) formaldehyde under vacuum for 15 to 30 min until the seedlings become water soaked and translucent, and Gly was added to a final concentration of 0.125 mol L^{-1} to quench the cross-linking. The seedlings were then ground to a powder in liquid nitrogen. The nuclei were isolated and lysed, and the chromatin solution was then sonicated to shear DNA into fragments of ~300 bp. The lysates were centrifuged at 12,000*g* for 5 min at 4°C, and the supernatant was incubated with anti-FLAG M2 magnetic beads (Sigma-Aldrich) to isolate the protein chromatin DNA complexes. The fragmental DNA was recovered after elution and reverse cross-linking and then purified using QIAquick PCR purification columns (Qiagen).

For the ChIP-seq analysis, libraries were prepared using DNAs obtained from the ChIP experiments using the TruSeq DNA LT/HT Sample Prep Kit (Illumina), following the manufacturer's instructions. The libraries were then sequenced to generate 50-bp single-end reads using a HiSeq2500 sequencer (Illumina) at RiboBio (Guangzhou, China). The raw reads were filtered using standard quality control measures and aligned to the rice genome (The IRGSP pseudomolecules, Build 4.0) using Bowtie2 version 2.2.5 software. Cross-correlation metrics were calculated using phantompeakqualtools (Landt et al., 2012). Peak calling was performed with MACS (http://liulab.dfci.harvard.edu/MACS/). Only uniquely mapped reads were used for peak identification, and OsSPL3 binding peaks were obtained by model-based analysis of ChIP-seq (Zhang et al., 2008) with default parameters. For all peaks identified in three replicates, if a peak in one replicate overlapped with any peak in either of the two other replicates, it was labeled as an overlapping peak; otherwise, it was labeled as a nonoverlapping peak. Homer software was used to annotate the ChIP-seq peaks and to identify differences between the wild type and *ProSPL3*:*smSPL3-FLAG* plants. The peaks were classified according to the following criteria: (1) peaks occurring within 3000 bp upstream of the TSS of a gene were classified as promoter region binding sites; (2) peaks localized within a gene body were further categorized as exon, intron, 5′ UTR, or 3′ UTR region binding sites; and (3) peaks not selected by the two preceding criteria were classified as intergenic region binding sites unless specified.

Immunoprecipitation Assays and Immunoblotting

Immunoprecipitation and immunoblotting assays were performed as described previously, with several modifications (Lv et al., 2014). Briefly, 5-d-old *ProSPL3*:*smSPL3-FLAG* seedlings were harvested, ground in liquid nitrogen, and resuspended in extraction buffer (50 mM Tris-MES, pH 8.0, 0.5 M Suc, 1 mM $MgCl_2$, 10 mM EDTA, and 5 mM DTT) with freshly added MG132 (50 μM) and 1× protease inhibitor cocktail (Roche). The SPL3-FLAG protein was enriched using anti-FLAG M2 magnetic beads (Sigma-Aldrich) and eluted using 3× FLAG peptide (Sigma-Aldrich). Next, an immunoblot analysis was performed using the anti-FLAG antibody produced in mouse (F1804, Sigma-Aldrich).

RNA-Seq Analysis

Total RNAs were isolated from the basal nodes (2 to 4 mm) of 3-d-old seedlings using a TRIzol kit (Thermo Fisher Scientific), according to the manufacturer's instructions. Samples from 50 seedlings were pooled as a biological repeat; three biological repeats were used per genotype. RNA quality was assessed using the Agilent Bioanalyzer. Illumina sequencing libraries were constructed following the manufacturer's protocol and then sequenced using an Illumina HisSeq2500 system at RiboBio. The remaining (clean) reads were mapped to the rice reference genome (Nipponbare) using Bowtie2 version 2.2.5 and TopHat (Trapnell et al., 2009). The reads per kilobase of transcript per million mapped reads method was used to calculate the unique gene expression levels according to the equation: reads per kilobase of transcript per million mapped reads = total $exon_{reads}$/mapped reads (millions) × exon length (kb). Cuffdiff (Trapnell et al., 2013) was used to determine the differential expression of genes. The false discovery rate was used to determine the threshold of P-values. The differentially expressed genes were screened with threshold criteria of false discovery rate < 0.05, P-value < 0.05, and fold change ≥ 2 and were divided into upregulated and downregulated transcripts. GO annotation analyses were completed using the BLAST2GO software (https://www.blast2go.com/), an automated tool for the assignment of GO terms. The functions of genes associated with the OsSPL3 binding sites and differentially expressed genes in the RNA-seq data sets were determined using these GO data sets.

Expression and Purification of Fusion Proteins

The full-length *OsSPL3* CDS was amplified from HJ2 cDNA and cloned in-frame into the 3′ terminus of glutathione S-transferase (GST) in pGEX-4T-1 (GE Healthcare). The primers used are listed in Supplemental Data Set 4. The GST-SPL3 fusion construct was transformed into *Escherichia coli* BL21 (DE3), and its expression was induced with 0.1 mM isopropyl-1-thio-D-galactopyranoside at 20°C for 16 h. The recombinant protein GST-SPL3

was purified using a Glutathione Sepharose 4 Fast Flow kit (GE Healthcare) and quantified using the Bio-Rad protein assay reagent and SDS-PAGE, as described previously (Wang et al., 2014).

Electrophoretic Mobility Shift Assay

EMSA was performed as described previously (Wang et al., 2014). The *OsMADS50* promoter fragment containing the GTAC motif was synthesized as a biotin-labeled oligonucleotide or an unlabeled oligonucleotide (competitor). The EMSA was performed using a LightShift Chemiluminescent EMSA kit (Thermo Fisher Scientific), according to the manufacturer's instructions. The migration of biotin-labeled probes was detected using the Chemiluminescent Nucleic Acid Detection Module (Thermo Fisher Scientific) and the ChemDoc XRS system (Bio-Rad). The oligonucleotide sequences are provided in Supplemental Data Set 4.

Transactivation Analysis in Plants

A transactivation analysis was performed in *N. benthamiana* plants, as described previously (Hellens et al., 2005). An ~4.0-kb DNA fragment spanning the OsSPL3 binding site in the *OsMADS50* promoter was amplified from HJ2 DNA and used to generate reporter plasmids (*ProMADS50:LUC*) containing the *OsMADS50* promoter and the *LUC* gene. The full-length *OsSPL3* CDS was amplified from HJ2 cDNA and then cloned into the pCAMBIA1300-35S vector to generate the effector plasmid *Pro35S:OsSPL3*. Luciferase assays were performed using the Dual-Luciferase Reporter Assay System (Promega). The primers used are listed in Supplemental Data Set 4.

Transcription Activation Assay in Yeast

The Matchmaker Gold Yeast Two-Hybrid System (Clontech) was used to test the transcription activation activity of *OsSPL3*. The full-length CDS and various truncated versions of *OsSPL3* were amplified from HJ2 cDNA and cloned into the pGBKT7 plasmid to produce in-frame fusions to the GAL4 DNA binding domain. Constructs were transformed into the yeast strain AH109 and selected on media lacking Trp. Yeast cells were grown at 30°C with shaking. The ability of the OsSPL3 protein to activate transcription in yeast was assayed by its ability to grow in the absence of His (conferred by the *HIS3* reporter gene).

GUS Histochemical and GFP Fluorescence Analysis

The histochemical GUS analysis was performed as described previously (Chen et al., 2013). Five-day-old seedlings were collected for the histochemical detection of *GUS* expression. The collected samples were incubated in the staining solution for 6 h at 37°C. Images were taken directly or using a stereomicroscope (Leica). Images of cross sections and longitudinal sections were taken using a microscope (Nikon) after cutting the sample into 40- to 80-μm sections using a microtome (Leica). For the GFP fluorescence analysis, the basal stems of 3 DAG *ProSPL3:GFP*, *ProSPL3:SPL3-GFP*, and *ProSPL3:smSPL3-GFP* transgenic seedlings were harvested and sectioned using a microtome. The sections were then imaged for GFP fluorescence using a LSM710 confocal laser scanning microscope (Zeiss), as described previously in Lv et al. (2014).

Exogenous IAA, NAA, and 6-BA Treatment

Germinated seeds were sown on floating nets and grown in hydroponic culture. After 6 d, the seedlings were transferred to the hydroponic culture with or without 10^{-6} M IAA, 10^{-6} M NAA, or 10^{-5} M 6-BA. Total RNA of stem bases was extracted after 0, 1, 3, 6, 12, and 24 h of treatment, and the expression of genes was analyzed by quantitative real-time PCR. For crown root number calculation, germinated seeds were sown on floating nets and grown in hydroponic culture containing 0, 10^{-13}, 10^{-11}, 10^{-9}, 10^{-7}, and 10^{-5} M IAA or NAA, respectively. Crown root numbers were recorded after 5 d of treatment with IAA or NAA.

Measurements of Phytohormones

Whole 5-d-old seedlings (100 mg) were ground to a powder in liquid nitrogen. The phytohormones were extracted from the powder at 4°C for 12 h with 1 mL of ethyl acetate that had been spiked with internal standards. The supernatant was collected after centrifugation (at 14,000*g*, 10 min, 4°C). The pellet was again extracted with 0.5 mL of ethyl acetate at 4°C for 1 h. The supernatant from the second extraction was collected and pooled with the first extraction. Supernatant was evaporated to dryness under N_2. The residue was resuspended in 0.1 mL of 50% (v/v) acetonitrile. After being centrifuged (at 14,000*g* and 4°C, for 10 min), the supernatant was then analyzed by HPLC-electrospray ionization-tandem mass spectrometry at Shanghai Applied Protein Technology Company (Shanghai, China). The mobile phase consisted of a combination of solvent A (0.05% [v/v] formic acid in water) and solvent B (0.05% [v/v] formic acid in acetonitrile). The linear gradient was as follows: 2 to 98% B (v/v) for 10 min, 2% B (v/v) for 10.1 min, and hold at 2% B to 13 min. The mass spectrometer (Qtrap 5500 System, AB Sciex) equipped with an electrospray ionization source was operated in positive/negative ionization and multiple reaction monitoring modes. The MS parameters were as follows: source temperature, 500°C; ion source gas 1, 45 psi; ion source gas 2, 45 psi; curtain gas, 30 psi; and ion spray voltage, 5500 V.

Statistical Analyses

The statistical analyses were performed using IBM SPSS Statistics. Student's two-tailed *t* tests were used to determine significant differences between two groups, while one-way analyses of variance (ANOVAs) with Tukey's honestly significant difference tests were used to determine significant differences among multiple data sets. The ANOVA and *t* test results are listed in Supplemental File.

Accession Numbers

Sequence data from this article can be found in the GenBank/EMBL databases under the following accession numbers: *OsSPL2* (Os01g0922600), *OsSPL3* (Os02g0139400), *OsSPL4* (Os02g0174100), *OsSPL7* (Os04g0551500), *OsSPL11* (Os06g0663500), *OsSPL12* (Os06g0703500), *OsSPL14* (Os08g0509600), *OsSPL16* (Os08g0531600), *OsMADS50* (Os03g0122600), *ARL1/CRL1* (Os03g0149100), *CRL4* (Os03g0666100), *OsIAA4* (Os01g0286900), *OsIAA5* (Os01g0675700), *OsIAA7* (Os02g0228900), *OsIAA9* (Os02g0805100), *OsIAA11* (Os03g0633500), *OsIAA13* (Os03g0742900), *OsIAA23* (Os06g0597000), *OsIAA31* (Os12g0601400), *OsARF1* (Os01g0236300), *OsARF5* (Os02g0141100), *OsARF13* (Os04g0690600), *OsARF19* (Os06g0702600), *OsARF22* (Os10g0479900), *OsPIN2* (Os06g0660200), *OsPIN5a* (Os01g0919800), *OsPIN5c* (Os09g0505400), *OsPIN10b* (Os05g0576900), and *OsACTIN1* (Os03g0718100).

Supplemental Data

Supplemental Figure 1. Phenotype and root gravitropic response of *lcrn1* in the Kasalath (Kas) background (*lcrn1*^{Kas}).

Supplemental Figure 2. Phenotype of *lcrn1* mutant plants.

Supplemental Figure 3. Sequences of *OsSPL3* cDNA and its deduced protein.

Supplemental Figure 4. Genomic differences in the *OsSPL3* genomic region between HJ2 and Kas, and the phenotype of the *OsmSPL3*^{Kas} transgenic plants.

Supplemental Figure 5. Transcript levels of OsmiR156 and *SPL* genes revealed by quantitative real-time PCR.

Supplemental Figure 6. Reverse transcription-PCR (RT-PCR) products in heterozygous plants.

Supplemental Figure 7. Phenotypes of *ProSPL3*:*SPL3-GFP* (*SPL3-GFP*) and *ProSPL3*:*smSPL3-GFP* (*smSPL3-GFP*) transgenic plants.

Supplemental Figure 8. Expression level of GAL4 BD fusion protein in yeast cells.

Supplemental Figure 9. Identification of *spl3-crispr* mutant plants and the phenotype of *spl3-crispr* plants.

Supplemental Figure 10. Phenotype of *ProSPL3*:*smSPL3-FLAG* transgenic plants *(smSPL3-FLAG*) and SPL3-FLAG protein enrichment using immunoprecipitation (IP).

Supplemental Figure 11. ChIP-seq analyses of the OsSPL3 binding sites.

Supplemental Figure 12. RNA-seq analysis of the *lcrn1* and wild-type (WT) plants.

Supplemental Figure 13. Expression pattern of *OsMADS50*, OsmiR156, and the *SPLs.* Revealed using quantitative real-time PCR.

Supplemental Figure 14. Phenotypes of the *OsMADS50*-overexpressing transgenic lines (*MADS50-OV*).

Supplemental Figure 15. Identification and phenotyping of the *mads50* mutant in the *lcrn1* genetic background at the flowering stage.

Supplemental Figure 16. Phenotype of the *mads50* mutant.

Supplemental Figure 17. Phenotypic characterization of the *lcrn1 arl1* double mutant.

Supplemental Figure 18. Expression of *OsSPL3* and *OsMADS50* in response to exogenous plant hormones IAA, NAA, and 6-BA and the content of auxin and cytokinin in wild-type, *lcrn1*, and two independent *OsMADS50*-overexpression transgenic lines.

Supplemental Table. Effect of exogenous auxin treatment on crown root number.

Supplemental Data Set 1. OsSPL3 binding sites identified in three ChIP-sequencing repetitions.

Supplemental Data Set 2. Differentially expressed genes between *lcrn1* and the wild type, revealed using RNA-seq.

Supplemental Data Set 3. Combined ChIP-seq and RNA-seq data.

Supplemental Data Set 4. Sequence of the primers and oligonucleotides used in this study.

Supplemental File. The results of statistical analyses.

ACKNOWLEDGMENTS

We thank Yaoguang Liu for providing the CRISPR/Cas9-related vectors. We thank Heven Sze for editing the article. We thank Jiming Xu for assisting with the measurements and Shelong Zhang for assisting with GFP imaging. This work was supported by the National Key Research and Development Program of China (grant 2016YFD0100700), the National Basic Research and Development Program of China (2015CB942900), the National Natural Science Foundation of China (grants 31572187 and 31372120), the Ministry of Agriculture of China (grant 2016ZX08001003-009), the Natural Science Foundation of Zhejiang Province, China (grant LZ17C020001), the Ministry of Education and Bureau of Foreign Experts of China (grant B14027), and the Fundamental Research Funds for the Central Universities (grant 2018FZA6002).

AUTHOR CONTRIBUTIONS

C.M. and Y.S. conceived and designed the experiments. Y.S., H.Z.Z., Y.W., H.Z., J.Z., Y.L., and Q.H. performed the experiments. Y.S., J.L., X.J., H.Y., and C.M. analyzed the data. Y.S. and C.M. wrote the article. All authors read and approved of the article.

Received January 18, 2019; revised March 8, 2019; accepted March 29, 2019; published April 2, 2019.

REFERENCES

Arora, R., Agarwal, P., Ray, S., Singh, A.K., Singh, V.P., Tyagi, A.K., and Kapoor, S. (2007). MADS-box gene family in rice: Genome-wide identification, organization and expression profiling during reproductive development and stress. BMC Genomics **8:** 242.

Aung, B., Gao, R., Gruber, M.Y., Yuan, Z.C., Sumarah, M., and Hannoufa, A. (2017). MsmiR156 affects global gene expression and promotes root regenerative capacity and nitrogen fixation activity in alfalfa. Transgenic Res. **26:** 541–557.

Axtell, M.J., and Bartel, D.P. (2005). Antiquity of microRNAs and their targets in land plants. Plant Cell **17:** 1658–1673.

Basheer-Salimia, R. (2007). Juvenility, maturity and rejuvenation in woody plants. Hebron Univ. Res. J. **3:** 17–43.

Birkenbihl, R.P., Jach, G., Saedler, H., and Huijser, P. (2005). Functional dissection of the plant-specific SBP-domain: Overlap of the DNA-binding and nuclear localization domains. J. Mol. Biol. **352:** 585–596.

Chen, X., Shi, J., Hao, X., Liu, H., Shi, J., Wu, Y., Wu, Z., Chen, M., Wu, P., and Mao, C. (2013). *OsORC3* is required for lateral root development in rice. Plant J. **74:** 339–350.

Chuck, G., Cigan, A.M., Saeteurn, K., and Hake, S. (2007). The heterochronic maize mutant *Corngrass1* results from overexpression of a tandem microRNA. Nat. Genet. **39:** 544–549.

Feng, S., Xu, Y., Guo, C., Zheng, J., Zhou, B., Zhang, Y., Ding, Y., Zhang, L., Zhu, Z., Wang, H., and Wu, G. (2016). Modulation of miR156 to identify traits associated with vegetative phase change in tobacco (*Nicotiana tabacum*). J. Exp. Bot. **67:** 1493–1504.

Gao, R., Wang, Y., Gruber, M.Y., and Hannoufa, A. (2018). miR156/SPL10 modulates lateral root development, branching and leaf morphology in Arabidopsis by silencing *AGAMOUS-LIKE 79.* Front. Plant Sci. **8:** 2226.

Garay-Arroyo, A., et al. (2013). The MADS transcription factor XAL2/AGL14 modulates auxin transport during Arabidopsis root development by regulating PIN expression. EMBO J. **32:** 2884–2895.

Hellens, R.P., Allan, A.C., Friel, E.N., Bolitho, K., Grafton, K., Templeton, M.D., Karunairetnam, S., Gleave, A.P., and Laing, W.A. (2005). Transient expression vectors for functional genomics, quantification of promoter activity and RNA silencing in plants. Plant Methods **1:** 13.

Inukai, Y., Sakamoto, T., Ueguchi-Tanaka, M., Shibata, Y., Gomi, K., Umemura, I., Hasegawa, Y., Ashikari, M., Kitano, H., and Matsuoka, M. (2005). *Crown rootless1*, which is essential for crown root formation in rice, is a target of an AUXIN RESPONSE FACTOR in auxin signaling. Plant Cell **17:** 1387–1396.

Jia, L., Wu, Z., Hao, X., Carrie, C., Zheng, L., Whelan, J., Wu, Y., Wang, S., Wu, P., and Mao, C. (2011). Identification of a novel mitochondrial protein, short postembryonic roots 1 (SPR1), involved in root development and iron homeostasis in *Oryza sativa.* New Phytol. **189:** 843–855.

Jiao, Y., Wang, Y., Xue, D., Wang, J., Yan, M., Liu, G., Dong, G., Zeng, D., Lu, Z., Zhu, X., Qian, Q., and Li, J. (2010). Regulation of *OsSPL14* by OsmiR156 defines ideal plant architecture in rice. Nat. Genet. **42:** 541–544.

Jun, N., Gaohang, W., Zhenxing, Z., Huanhuan, Z., Yunrong, W., and Ping, W. (2011). OsIAA23-mediated auxin signaling defines postembryonic maintenance of QC in rice. Plant J. **68:** 433–442.

Kitomi, Y., Ogawa, A., Kitano, H., and Inukai, Y. (2008). *CRL4* regulates crown root formation through auxin transport in rice. Plant Root **2:** 19–28.

Kitomi, Y., Ito, H., Hobo, T., Aya, K., Kitano, H., and Inukai, Y. (2011). The auxin responsive AP2/ERF transcription factor *CROWN ROOTLESS5* is involved in crown root initiation in rice through the induction of *OsRR1*, a type-A response regulator of cytokinin signaling. Plant J. **67:** 472–484.

Klein, J., Saedler, H., and Huijser, P. (1996). A new family of DNA binding proteins includes putative transcriptional regulators of the *Antirrhinum majus* floral meristem identity gene *SQUAMOSA.* Mol. Gen. Genet. **250:** 7–16.

Landt, S.G., et al. (2012). ChIP-seq guidelines and practices of the ENCODE and modENCODE consortia. Genome Res. **22:** 1813–1831.

Lee, J., Park, J.J., Kim, S.L., Yim, J., and An, G. (2007). Mutations in the rice liguleless gene result in a complete loss of the auricle, ligule, and laminar joint. Plant Mol. Biol. **65:** 487–499.

Liu, H., Wang, S., Yu, X., Yu, J., He, X., Zhang, S., Shou, H., and Wu, P. (2005). ARL1, a LOB-domain protein required for adventitious root formation in rice. Plant J. **43:** 47–56.

Liu, S., Wang, J., Wang, L., Wang, X., Xue, Y., Wu, P., and Shou, H. (2009). Adventitious root formation in rice requires OsGNOM1 and is mediated by the OsPINs family. Cell Res. **19:** 1110–1119.

Llave, C., Xie, Z., Kasschau, K.D., and Carrington, J.C. (2002). Cleavage of *Scarecrow-like* mRNA targets directed by a class of *Arabidopsis* miRNA. Science **297:** 2053–2056.

Lv, Q., Zhong, Y., Wang, Y., Wang, Z., Zhang, L., Shi, J., Wu, Z., Liu, Y., Mao, C., Yi, K., and Wu, P. (2014). SPX4 negatively regulates phosphate signaling and homeostasis through its interaction with PHR2 in rice. Plant Cell **26:** 1586–1597.

Machanick, P., and Bailey, T.L. (2011). MEME-ChIP: Motif analysis of large DNA datasets. Bioinformatics **27:** 1696–1697.

Marcon, C., Paschold, A., and Hochholdinger, F. (2013). Genetic control of root organogenesis in cereals. Methods Mol. Biol. **959:** 69–81.

Massoumi, M., Krens, F.A., Visser, R.G., and De Klerk, G.M. (2017). Azacytidine and miR156 promote rooting in adult but not in juvenile *Arabidopsis* tissues. J. Plant Physiol. **208:** 52–60.

Miura, K., Ikeda, M., Matsubara, A., Song, X.J., Ito, M., Asano, K., Matsuoka, M., Kitano, H., and Ashikari, M. (2010). *OsSPL14* promotes panicle branching and higher grain productivity in rice. Nat. Genet. **42:** 545–549.

Rogers, E.D., and Benfey, P.N. (2015). Regulation of plant root system architecture: Implications for crop advancement. Curr. Opin. Biotechnol. **32:** 93–98.

Si, L., et al. (2016). *OsSPL13* controls grain size in cultivated rice. Nat. Genet. **48:** 447–456.

Smith, S., and De Smet, I. (2012). Root system architecture: insights from *Arabidopsis* and cereal crops. Philos. Trans. R. Soc. Lond. B Biol. Sci. **367:** 1441–1452.

Sun, C.H., Yu, J.Q., Duan, X., Wang, J.H., Zhang, Q.Y., Gu, K.D., Hu, D.G., and Zheng, C.S. (2018). The MADS transcription factor CmANR1 positively modulates root system development by directly regulating *CmPIN2* in chrysanthemum. Hortic. Res. **5:** 52.

Trapnell, C., Pachter, L., and Salzberg, S.L. (2009). TopHat: Discovering splice junctions with RNA-seq. Bioinformatics **25:** 1105–1111.

Trapnell, C., Hendrickson, D.G., Sauvageau, M., Goff, L., Rinn, J.L., and Pachter, L. (2013). Differential analysis of gene regulation at transcript resolution with RNA-seq. Nat. Biotechnol. **31:** 46–53.

Varkonyi-Gasic, E., Wu, R., Wood, M., Walton, E.F., and Hellens, R.P. (2007). Protocol: A highly sensitive RT-PCR method for detection and quantification of microRNAs. Plant Methods **3:** 12.

Wang, Z., et al. (2014). Rice SPX1 and SPX2 inhibit phosphate starvation responses through interacting with PHR2 in a phosphate-dependent manner. Proc. Natl. Acad. Sci. USA **111:** 14953–14958.

Wang, J.W., Czech, B., and Weigel, D. (2009). miR156-regulated SPL transcription factors define an endogenous flowering pathway in *Arabidopsis thaliana.* Cell **138:** 738–749.

Wang, J.W., Park, M.Y., Wang, L.J., Koo, Y., Chen, X.Y., Weigel, D., and Poethig, R.S. (2011a). miRNA control of vegetative phase change in trees. PLoS Genet. **7:** e1002012.

Wang, L., Guo, M., Li, Y., Ruan, W., Mo, X., Wu, Z., Sturrock, C.J., Yu, H., Lu, C., Peng, J., and Mao, C. (2018a). *LARGE ROOT ANGLE1*, encoding OsPIN2, is involved in root system architecture in rice. J. Exp. Bot. **69:** 385–397.

Wang, Q.L., Sun, A.Z., Chen, S.T., Chen, L.S., and Guo, F.Q. (2018b). SPL6 represses signalling outputs of ER stress in control of panicle cell death in rice. Nat. Plants **4:** 280–288.

Wang, S., Wu, K., Yuan, Q., Liu, X., Liu, Z., Lin, X., Zeng, R., Zhu, H., Dong, G., Qian, Q., Zhang, G., and Fu, X. (2012). Control of grain size, shape and quality by *OsSPL16* in rice. Nat. Genet. **44:** 950–954.

Wang, X.F., He, F.F., Ma, X.X., Mao, C.Z., Hodgman, C., Lu, C.G., and Wu, P. (2011b). OsCAND1 is required for crown root emergence in rice. Mol. Plant **4:** 289–299.

White, P.J., George, T.S., Gregory, P.J., Bengough, A.G., Hallett, P.D., and McKenzie, B.M. (2013). Matching roots to their environment. Ann. Bot. **112:** 207–222.

Xie, K., Wu, C., and Xiong, L. (2006). Genomic organization, differential expression, and interaction of SQUAMOSA promoter-binding-like transcription factors and microRNA156 in rice. Plant Physiol. **142:** 280–293.

Xu, M., Zhu, L., Shou, H., and Wu, P. (2005). A PIN1 family gene, OsPIN1, involved in auxin-dependent adventitious root emergence and tillering in rice. Plant Cell Physiol. **46:** 1674–1681.

Xu, M., Hu, T., Zhao, J., Park, M.Y., Earley, K.W., Wu, G., Yang, L., and Poethig, R.S. (2016). Developmental functions of miR156-regulated *SQUAMOSA PROMOTER BINDING PROTEIN-LIKE* (*SPL*) genes in *Arabidopsis thaliana.* PLoS Genet. **12:** e1006263.

Xu, X., Li, X., Hu, X., Wu, T., Wang, Y., Xu, X., Zhang, X., and Han, Z. (2017). High miR156 expression is required for auxin-induced adventitious root formation via *MxSPL26* independent of *PINs* and *ARFs* in *Malus xiaojinensis.* Front. Plant Sci. **8:** 1059.

Yan, W., Chen, D., and Kaufmann, K. (2016). Molecular mechanisms of floral organ specification by MADS domain proteins. Curr. Opin. Plant Biol. **29:** 154–162.

Yang, J., Gao, M.X., Hu, H., Ding, X.M., Lin, H.W., Wang, L., Xu, J.M., Mao, C.Z., Zhao, F.J., and Wu, Z.C. (2016). OsCLT1, a CRT-like transporter 1, is required for glutathione homeostasis and arsenic tolerance in rice. New Phytol. **211:** 658–670.

Yu, C., Liu, Y., Zhang, A., Su, S., Yan, A., Huang, L., Ali, I., Liu, Y., Forde, B.G., and Gan, Y. (2015). MADS-box transcription factor

OsMADS25 regulates root development through affection of nitrate accumulation in rice. PLoS One **10:** e0135196.

Yu, L.H., Miao, Z.Q., Qi, G.F., Wu, J., Cai, X.T., Mao, J.L., and Xiang, C.B. (2014). MADS-box transcription factor AGL21 regulates lateral root development and responds to multiple external and physiological signals. Mol. Plant **7:** 1653–1669.

Zhang, X., Zou, Z., Zhang, J., Zhang, Y., Han, Q., Hu, T., Xu, X., Liu, H., Li, H., and Ye, Z. (2011). Over-expression of sly-miR156a in tomato results in multiple vegetative and reproductive trait alterations and partial phenocopy of the *sft* mutant. FEBS Lett. **585:** 435–439.

Zhang, Y., Liu, T., Meyer, C.A., Eeckhoute, J., Johnson, D.S., Bernstein, B.E., Nusbaum, C., Myers, R.M., Brown, M., Li, W., and Liu, X.S. (2008). Model-based analysis of ChIP-seq (MACS). Genome Biol. **9:** R137.

Zhao, Y., Hu, Y., Dai, M., Huang, L., and Zhou, D.X. (2009). The WUSCHEL-related homeobox gene *WOX11* is required to activate shoot-borne crown root development in rice. Plant Cell **21:** 736–748.

Zhao, Y., Cheng, S., Song, Y., Huang, Y., Zhou, S., Liu, X., and Zhou, D.X. (2015). The interaction between rice ERF3 and WOX11 promotes crown root development by regulating gene expression involved in cytokinin signaling. Plant Cell **27:** 2469–2483.

Zhu, Q.L., Yang, Z.F., Zhang, Q.Y., Chen, L.T., and Liu, Y.G. (2014). Robust multi-type plasmid modifications based on isothermal in vitro recombination. Gene **548:** 39–42.